

UNIVERSITY OF THE WITWATERSRAND
Johannesburg



NATURE AND DURATION OF MID-CRUSTAL
GRANULITE FACIES METAMORPHISM
AND CRUSTAL GROWTH : EVIDENCE FROM
SINGLE ZIRCON U-PB GEOCHRONOLOGY
IN NAMAQUALAND, SOUTH AFRICA

L. J. ROBB, R. A. ARMSTRONG and D. J. WATERS

INFORMATION CIRCULAR No. 323

UNIVERSITY OF THE WITWATERSRAND
JOHANNESBURG

**NATURE AND DURATION OF MID-CRUSTAL GRANULITE FACIES
METAMORPHISM AND CRUSTAL GROWTH : EVIDENCE FROM SINGLE
ZIRCON U-PB GEOCHRONOLOGY IN NAMAQUALAND, SOUTH AFRICA**

by

L. J. ROBB¹, R. A. ARMSTRONG² and D. J. WATERS³

(¹ Department of Geology, University of the Witwatersrand, P/Bag 3, P.O.WITS 2050,
South Africa; ² Research School of Earth Sciences, The Australian National
University, Canberra, Australia; and ³ Department of Earth Sciences, University of
Oxford, Oxford, UK)

**ECONOMIC GEOLOGY RESEARCH UNIT
INFORMATION CIRCULAR No. 323**

May, 1998

**NATURE AND DURATION OF MID-CRUSTAL GRANULITE
FACIES METAMORPHISM AND CRUSTAL GROWTH:
EVIDENCE FROM SINGLE ZIRCON U-PB GEOCHRONOLOGY IN
NAMAQUALAND, SOUTH AFRICA**

ABSTRACT

The Namaqualand Metamorphic Complex is a well-exposed, Mesoproterozoic, low pressure, amphibolite-granulite facies terrane flanking the Archaean Kaapvaal Craton of southern Africa. Published isotopic dating in the region suggests a prolonged interval of prograde granulite facies metamorphism and episodic granite emplacement in the mid-crust. In contrast, thermal modelling, which attempts to accommodate the large amount of heat required for mid-crustal granulite grade mineral reactions and the isobaric cooling path, suggests a mechanism of sub- and superjacent magmatic accretion during an event that should not have exceeded 30 million years in duration. Resolution of this enigma is provided by precise U-Pb zircon SHRIMP dating of the major orthogneissic units of the region. These data point to a period of Kibaran crustal growth at 1220-1170 Ma which occurred on the margins of a Palaeoproterozoic (2000-1800 Ma) continental nucleus. A later, distinct, orogenic episode, here termed the Namaquan (equivalent to the Grenvillian), involved crustal thickening and magmatism at 1060-1030 Ma and was responsible for, and coeval with, the peak of metamorphism. Low-P granulite facies metamorphism in the region is, therefore, the result of advective introduction of heat and crustal thickening by magmatic accretion over a relatively short, 30 million year, time interval.

—oOo—

**NATURE AND DURATION OF MID-CRUSTAL GRANULITE
FACIES METAMORPHISM AND CRUSTAL GROWTH:
EVIDENCE FROM SINGLE ZIRCON U-Pb GEOCHRONOLOGY IN
NAMAQUALAND, SOUTH AFRICA**

CONTENTS

	Page
INTRODUCTION	1
The mid-crustal granulite facies problem	1
The study area	2
Lithostratigraphy of the OCD	3
Structure	3
Metamorphism	5
SHRIMP U-Pb Zircon AGE DETERMINATIONS	6
Sampling	6
Analytical procedure	6
Zircon morphology, U-Th contents and recognition of magmatic-metamorphic growth	8
Zircon U-Pb isotope data	11
Gladkop Suite (NAM6 and NAM7)	11
Little Namaqualand Suite (NAM1 and NAM2) and	
Two-pyroxene Granulite (NAM3)	12
Spektakel Suite (NAM4 and NAM8)	17
Koperberg Suite (NAM9, NAM10 and NAM11)	20
DISCUSSION AND CONCLUSIONS	24
Events in the Okiep Copper District	24
Crustal growth	27
P-T-t path	29
Causes of granulite facies metamorphism in the mid-crust	31
ACKNOWLEDGEMENTS	33
REFERENCES	33
APPENDIX	38

____ oOo ____

Published by the Economic Geology Research Unit
Department of Geology
University of the Witwatersrand
1 Jan Smuts Avenue
Johannesburg 2001
South Africa

ISBN 1-86838-210-9

NATURE AND DURATION OF MID-CRUSTAL GRANULITE FACIES METAMORPHISM AND CRUSTAL GROWTH: EVIDENCE FROM SINGLE ZIRCON U-Pb GEOCHRONOLOGY IN NAMAQUALAND, SOUTH AFRICA

INTRODUCTION

The mid-crustal granulite facies problem

Granulite facies terranes record segments of the earth's lower and middle crust, in which rocks that equilibrated at high pressures (P) and temperatures (T), are preserved. They exhibit a wide variety of petrogenetic features and a complex secular evolution which often preserves both prograde and retrograde characteristics. They formed in response to a number of different crustal and tectonic processes and, consequently, their origin is important in understanding the nature of continental growth and crustal evolution.

Granulites typically reflect P-T conditions in the range 6-9kb and 750-850°C and comprise anhydrous mineral assemblages that point to conditions of reduced water activity (aH_2O). In the lower crust granulites commonly represent the residues of a partial melting event which moves melt and volatiles to higher crustal levels. Alternatively, granulites may form in zones where mutually soluble CO₂-H₂O rich fluids stream upwards through the crust causing localised reduction in volatile content and accompanying mineral phase changes along the fluid channelway. In the mid-crust, however, the formation of low- to intermediate-P granulites require fairly specific mechanisms requiring high heat flow and transient elevation of local geothermal gradients. Another problem related to the mechanisms of granulite formation in general, is the longevity of the metamorphic pulse. Isotopic age determinations, the errors on which are commonly of the same order as the duration of the event itself, have indicated that the prograde granulite facies event might reflect a prolonged period of thermal perturbation lasting for as much as 100-200 million years. In the Arunta Block of the Reynolds Range, central Australia, metamorphism is believed to have lasted for some 110 million years (Dirks and Wilson, 1990; Dirks et al. 1991), while in the Namaqualand Metamorphic Complex of South Africa, Clifford et al.(1994) have suggested that granulite facies metamorphism spanned some 150 million years, between 1200 and 1050 Ma. In the mid-crust, in particular, a difficulty with the notion of long-lived metamorphic scenarios revolves around the maintenance of abnormally high thermal gradients for such lengthy periods of geologic time. In Namaqualand, for example, it has been argued (Waters, 1989; 1990) that peak metamorphic conditions could be attained through processes of magmatic accretion. Thermal modelling suggested that this could have been achieved by a (maximum 30km thick) basaltic underplate at least 10km below the present level of erosion, accompanied by another 10km of acid intrusions into the mid-crust. Given the constraints imposed by the cooling rates of the accreted magmas, the duration of the thermal maximum should not have exceeded 30 million years.

The present paper examines the secular relationships between crustal growth and metamorphism in a well-studied low-P granulite terrane, represented by the Mesoproterozoic Namaqualand Metamorphic Complex (NMC). The ages of major crust forming events and the timing and duration of metamorphism are examined through high-precision U -Pb isotopic age determinations on a variety of rock types from the Okiep Copper District in the NMC. Inferences are then made regarding the origin of granulite facies metamorphism in this section of the mid-crust.

The study area

The Okiep Copper District (OCD) is a well-known area for copper production in the Northern Cape Province of South Africa, having flourished as a mining district for some 140 years. It is located in the NMC which forms part of an extensive orogenic belt of mid- to late-Proterozoic age which girdles the southern limit of the Kaapvaal Craton in southern Africa (Fig. 1). Extensions of this orogenic belt occur elsewhere in Africa, where they are referred to as the Kibaran Orogeny* (Clifford, 1970; Thomas et al., 1994), and this in turn is analogous to similar zones of high-grade metamorphic rocks elsewhere in the world which are generally referred to as Grenvillian* (Clifford et al., 1981). The NMC is a classic locality for the demonstration of low-P granulite facies metamorphism and the P-T regime that prevails in the area has been well studied (Clifford et al., 1975; 1981; Waters, 1988; 1989; 1990). The OCD in particular, has been mapped in great detail and the regional lithostratigraphy well documented in numerous publications (see recent review in Lombaard et al., 1986).

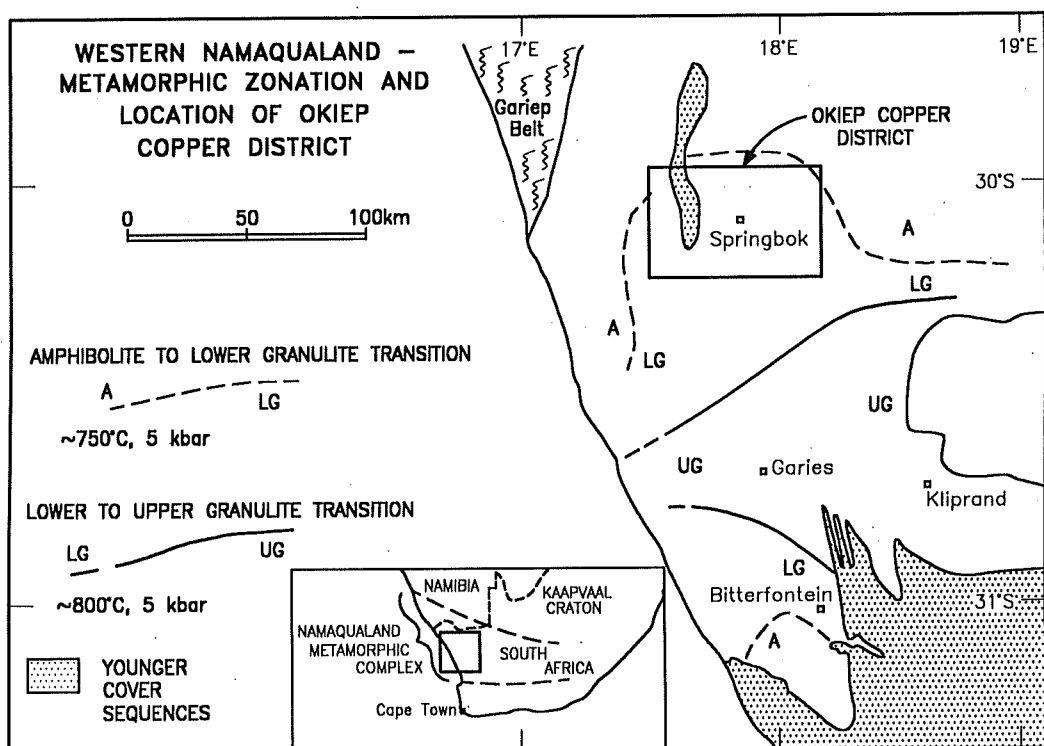


Fig. 1: Location of the study area and simplified representation of the metamorphic zonation in western Namaqualand.

The structural evolution of the OCD and surrounds has likewise been studied in great detail (Blignault et al., 1983; Joubert, 1971) and recently placed into the broader context of Kibaran tectonic evolution in the review of Thomas et al. (1994). In brief, the NMC outcrops

* Although the term "Kibaran" has been applied to Mesoproterozoic orogenic terranes in many parts of Africa, it is generally accepted that within the Kibaran Belt of Central Africa, rock ages, although poorly constrained, tend to occur in the range 1400 - 1200 Ma. This orogeny differs from those where rocks formed at 1100 - 1000 Ma, which are globally referred to as "Grenvillian". In the present study the latter will be referred to as "Namaquan" to accentuate their geographical context and in keeping with the recommendations of Tack et al. (1993) and Thomas et al. (1994).

over an extensive area of some 30 000 km², forming part of a mid- to late-Proterozoic continent-wide orogenic cycle. It also extends into, and forms part of the crust-forming processes involved in the assembly of the Rodinian supercontinent (Hoffman, 1992). The NMC is a polymetamorphic terrane and preserves remnants of an older, Palaeoproterozoic (2000–1800 Ma) orogenic cycle in addition to the Kibaran crust-forming events. This older orogenic cycle is here referred to as the Kheisian (Hartnady et al., 1995) and is probably analogous to the Ubendian Orogeny of central Africa. A major pulse of sedimentation (the Okiep Group) was deposited on the Kheisian basement and was subsequently deformed and metamorphosed during the Kibaran Orogeny. In addition the western coastal strip of the NMC appears to have been tectonically and thermally disturbed by an early Pan-African overprint. The OCD is mainly underlain by syn-tectonic orthogneisses and late-tectonic granitoids which intrude into remnants of the Kheisian basement and the Okiep Group.

Crustal components which formed during the Kheis Orogeny appear to have been accreted to the Archaean Kaapvaal Craton to form a cohesive continental fragment prior to the deposition of pre- or early-Kibaran supracrustal sequences (Thomas et al., 1994). The Kibaran Orogeny itself appears to have been initiated by rifting of existing continental margins to form incipient oceanic basins and back-arc or extensional intracratonic basin sedimentation. The extensional regime was followed by a convergent phase, arising from collision of the continent (which acted as a south-west-directed indentor) with the early Kibaran supracrustal sequences. This resulted in voluminous granitoid magmatism associated with crustal shortening and low-angle foreland thrusting/shearing (Jacobs et al., 1993).

Lithostratigraphy of the OCD

The long-lived crustal pre-history and intense deformation of the NMC means that regional lithostratigraphic interpretation and correlation is extremely difficult. In the OCD, however, the programme of detailed mapping and copper exploration over many decades has resulted in a reasonable understanding of the sequence of geological events in the area. In the western NMC, two major lithostratigraphic units are recognised (after Blignault et al., 1983); these are divided into volcanic-sedimentary successions and intrusive sequences and, together with previously published age determinations, are summarised in Table 1.

In brief, the western NMC comprises a complex succession of multiply-deformed rock types of two principal ages; a Kheisian core is preserved in a little-deformed region known as the Orange River igneous belt, in which calc-alkaline magmatism took place between circa 2000 and 1800 Ma. Between this region and the OCD an extensive area of granitic orthogneisses at amphibolite grade is preserved, and this crust also appears to have formed during the Kheis Orogeny, in this case at around 1820 Ma. These rocks were superseded by Kibaran sediments and intrusive granitoids, which were generated and subsequently buried between about 1300–1000 Ma.

Structure

At least three distinct increments of deformation can be recognised as being relevant to the magmatic and metamorphic evolution of the OCD, in addition to the late brittle faulting which displaces all the rocks of the region. An early D₁ deformation is expressed as intrafolial folds within orthogneisses of the Gladkop Suite and metasedimentary xenolithic remnants

Table 1: Lithostratigraphy and existing chronology in the Okiep Copper District and environs

VOLCANOSEDIMENTARY SUCCESIONS

Orange River Sequence - a composite calc-alkaline igneous province comprising an older (1996 ± 15 Ma) extrusive component (the Orange River Group; Reid, 1979) and younger (1900 ± 30 , 1830 ± 30 and 1731 ± 20 Ma) intrusive granitoids (the Violsdrif Suite; Reid, 1979; SACS, 1980; Welke et al., 1979).

Grunau Sequence - a monotonous metashale/wacke assemblage, in places interbedded with volcanics of the Orange River Group.

Aggeneys Sequence - a compositionally variable sequence of metasediments comprising chemogenic units, meta-arenites and minor intercalated volcanic rocks. Two geographically distinct units are recognized, each with their own local characteristics. These are:-

(i) Bushmanland Group in eastern NMC, which includes the ferruginous quartzite, shale, calc-silicate assemblages and amphibolite (1649 ± 90 Ma; Reid et al., 1987); also the associated Pb -Zn -Ag massive sulphide mineralization at Aggeneys and Gamsberg (dated at ca. 1300 Ma; Köppel, 1980); and

(ii) Okiep Group, which incorporates the Een Riet, Khurisberg, Aardvark, Garies and Bitterfontein Subgroups of the western NMC.

INTRUSIONS

Gladkop Suite - an extensive suite of grey-pink orthogneisses developed between the OCD and the Orange River Sequence. At least three sub-units are recognized; fine-grained, granodioritic Steinkopf gneiss, intruded by the coarser, K-feldspar megacrystic Brandewynsbank gneiss, which is in turn intruded by the leucocratic Noenoemaasberg gneiss (1824 ± 70 Ma; Barton, 1983).

Little Namaqualand Suite - an extensively developed, augen-textured suite of granitic orthogneisses. Two sub-units are defined in the OCD, these are the Nababeep gneiss (1179 ± 28 Ma; Barton, 1983; 1223 ± 48 Ma; Clifford et al., 1994), which is intruded by the Modderfontein gneiss.

Spektakel Suite - a widely developed suite of largely massive, K-felspar megacrystic granitoids. Three components have been identified; the Concordia granite which has a well-developed lineation in places; the Rietberg granite which occurs only locally in the NW of the OCD and intrudes the Concordia granite (1105 ± 24 Ma; Clifford et al., 1994); and the Kweekfontein granite suite, irregular dyke/sill-like intrusions which are distinctly post-tectonic.

Koperberg Suite - a multi-component suite of sill/dyke like intrusions which are generally emplaced along cusp-like antiformal structures. Some 1700 of these intrusions have been identified in the OCD and their lithologies include andesine anorthosite (1029 ± 10 Ma; Clifford et al., 1994), biotite diorite, leuconorite, norite and hypersthenite. Widely distributed Cu (bornite-chalcocite-chalcopyrite) mineralization is related to the later mafic components of the suite.

(Joubert, 1971; Blignault et al., 1983). This deformation may be a remnant of the Kheis orogenic cycle at 2000-1800 Ma. The most pervasive deformation recognised in the OCD (the D₂ event) is manifest as a widespread subhorizontal gneissosity which is typically evident within, and must therefore post-date, the orthogneisses of the Little Namaqualand Suite. This deformation is responsible for the formation of augen textures in these gneisses and is also evident as large and small scale isoclinal folds in the Springbok quartzite. The stresses associated with D₂ deformation persisted until the onset of Spektakel Suite intrusion as the Concordia granite occasionally displays a weakly developed gneissosity, particularly along the basal portions of the sheet. The Rietberg and Kweekfontein components of the suite are, however, post-D₂. The notion that the D₂ event is represented by a single, long-lived period of compression has been challenged by Raith and Harley (1997) who now recognise discrete D_{2a} and D_{2b} events, separated in time by a period in excess of 100 million years.

A subsequent compressional, N-S directed, D₃ event resulted in the formation of regional, kilometre-scale wavelength, open folds which deform the subhorizontal D₂ fabric. On a smaller scale this deformation also resulted in the development of complex, E-W trending kink folds, often manifest as anticlines or monoclines (Kisters et al., 1994). These structures, referred to locally as "steep structures" because they rotate the regional subhorizontal fabric into a subvertical attitude, are economically important as they host many of the cupriferous Koperberg Suite intrusions. Steep structures are well developed in the Little Namaqualand and lower Spektakel Suites, but are virtually absent in the upper part of the Concordia sheet and Rietberg granite. Intrusion of the Koperberg Suite is nevertheless syn- to late-tectonic with respect to the D₃ deformation as the intrusions exhibit planar fabrics, metamorphic annealing and folded cumulate layering (Kisters et al., 1994). Koperberg Suite intrusions within the Little Namaqualand Suite and lower Concordia granite sheet tend to exhibit steep structure controlled emplacement and dyke/sill-like geometries. Intrusions within the stratigraphically higher portions of the Concordia sheet and Rietberg granite have plug-like geometries and their emplacement is controlled by buoyancy and thermal erosion.

Metamorphism

Most metamorphic studies in the NMC have concentrated on supracrustal rocks where mineral assemblages in metapelites and metabasites have provided reliable constraints on the P-T-time evolution of the terrane (Clifford et al., 1975a,b; 1981; Waters, 1989; 1990; 1991). Regional studies have defined a symmetry in metamorphic zonation (Waters 1986), whereby the widespread development of amphibolite-grade rocks typical of most of the Bushmanland Subprovince (east of the OCD), merges into a core of lower-granulite and eventually upper-granulite grades centred around Garies-Kliprand (Fig. 1). The diagnostic amphibolite facies assemblage in many of the rock types over much of the terrane comprises biotite + sillimanite + quartz. The OCD falls into a region of lower-granulite grade (Fig. 1) where metabasite assemblages comprise Opx + Cpx + Pl + Hbl and metapelites are dominated by Crd + Grt + Kfs + Qtz (often with leucocratic segregation of Grt + Kfs). The upper-granulite grade zone to the south of the OCD is characterised by hercynitic spinel + quartz and rare osumilite assemblages in metapelites.

Mineral thermometers and barometers allow the estimation of P-T conditions to be made as a function of consecutive increments of mineral growth and deformation (Waters, 1989). The prograde transformation from amphibolite to granulite grade is recognised from

with a low-pressure amphibolite grade (circa 700°C and 4kb). Further evidence for the prograde amphibolite to granulite transition is derived from the formation of partial melts in metapelites by dehydration of biotite rather than muscovite. Further increases in pressure and temperature are recorded by the presence of garnet- and sapphirine-forming reactions which identify granulite grades at around 750-800°C and 3-5.5kb. Peak metamorphic conditions are recorded by the growth of hercynite + quartz at the expense of cordierite, and the formation of osumilite in metapelites. Peak conditions probably reached circa 850-900°C and 4-6kb. The retrograde P-T path for the NMC is recorded by the development of coronas around earlier metamorphic minerals. Cordierite or sillimanite overgrowths around hercynitic spinel and the replacement of cordierite by garnet + biotite/sillimanite suggest cooling at constant or even slightly increased pressures (Waters, 1989). Certainly pressures did not decrease significantly until below 600°C, a feature which suggests an anti-clockwise P-T-t path for the NMC.

The timing of metamorphism, especially in absolute terms, is more difficult to constrain accurately. Prograde mineral growth post-dated and/or outlasted the principal D₂ period of deformation in the NMC and appears to have been synchronous with the open-fold D₃ deformation (Waters, 1989). Evidence for this is provided by the development of coarse cordierite and garnet overgrowths on sillimanite which defines the regional D₂ fabric, as well as melt segregations which also obliterate this fabric. Clifford et al. (1975; 1981; 1994) have suggested that the age of the prograde metamorphic peak is reflected in the Rb-Sr errorchron of the Nababeep gneiss (ca. 1200 Ma; Table 1) and that this peak condition prevailed until the intrusion of the Koperberg Suite at 1030 Ma. Waters (1989), however, argued that D₂ occurred under amphibolite facies conditions and that attainment of granulite grades was only achieved in late- or post-D₂ times. This problem is discussed again later in the context of the data presented in the present study.

SHRIMP U -Pb ZIRCON AGE DETERMINATIONS

Sampling

Samples were collected over a fairly restricted area within the OCD to ensure, as far as possible, that the rocks analysed had all been subjected to similar metamorphic histories. Samples were selected to be representative of the major lithostratigraphic units of the region and their distribution is illustrated in Figure 2. A description of the samples and more detailed localities are provided in the Appendix.

Analytical procedure

Samples of between 1-2 kg in mass were subjected to routine heavy mineral separation which involved crushing and subsequent Wifley Table, heavy liquid and Frantz magnetic separation. Zircons were hand-picked for representativity and then mounted in epoxy and polished. Individual zircon grains were subjected to U-Pb isotopic analysis using the Sensitive High Resolution Ion Microprobe (SHRIMP II) developed at the Research School of Earth Sciences at The Australian National University, Canberra, Australia.

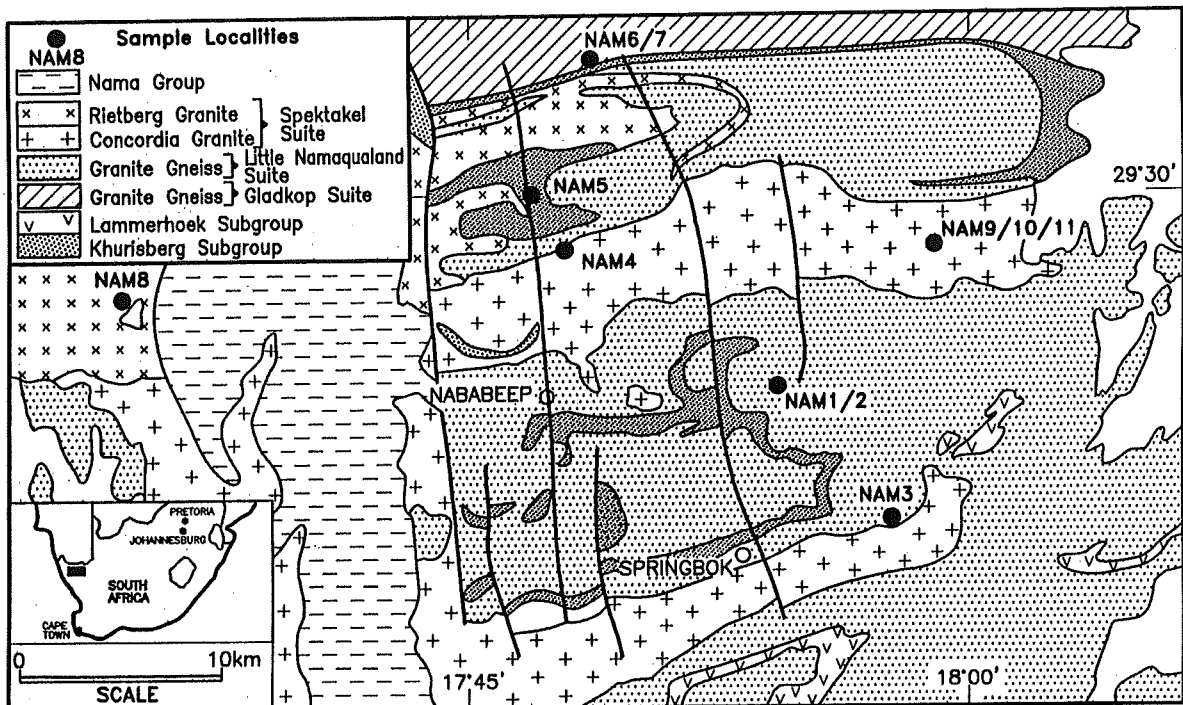


Fig.2: Simplified geological map of the Okiep Copper District and the location of samples analysed in the present study. Sample description and localities provided in Appendix.

Detailed analytical procedures on the SHRIMP are reported in Compston et al. (1984) and Williams and Claesson (1987). Briefly, the SHRIMP technique focuses a primary beam of negative oxygen ions *in vacuo* onto the zircon surface, from which a small area (25-30 μm diameter) of sputtered positive secondary ions is extracted. Secondary ions, which include Zr, Th, U and Pb from the zircon are passed through a curvilinear flight path in a strong magnetic field and then counted at a mass resolution of 6500 on a single collector using cyclic magnetic stepping. Isotopic ratios and inter-element fractionation were monitored by continuous reference to a standard Sri Lankan zircon (SL13), fragments of which were mounted with each sample. Progressive changes in the Pb/U ionic ratio during sputtering was compensated for by using an empirical quadratic relationship between Pb^+/U^+ and UO^+/U^+ determined for the standard zircon. A radiogenic $^{206}\text{Pb}/^{238}\text{U}$ ratio of 0.0928 for the standard zircon, corresponding to an age of 572 Ma was obtained through standard isotope dilution analysis. Initial Pb isotope compositions of the analysed zircons are assumed to be similar to that of model-derived average crustal Pb of similar age according to Cumming and Richards (1975).

The analytical precision of Pb isotope ratios is controlled by machine counting statistics while that in Pb/U ratios is affected by uncertainties in the standard calibration. Ages were calculated using the recommended Steiger and Jäger (1977) decay constants. Weighted mean $^{207}\text{Pb}/^{206}\text{Pb}$ ages were obtained for zircons exhibiting an obvious clustering and indistinguishable $^{207}\text{Pb}/^{206}\text{Pb}$ ages at a 95% confidence level (i.e. $t\sigma$, where t is the Fisher's t). Individual analyses in the data tables and concordia diagrams are presented at 1σ . Errors associated with scatter within the cluster are obtained by standard statistical techniques. Dispersion within the cluster is attributed to modern Pb loss. Analyses which do not fall within the clusters of weighted mean ages cannot be interpreted unambiguously and are considered to reflect uncertainties caused by ancient Pb loss or overlap of the ion beam onto domains of the zircon crystal with different isotopic ratios/ages.

Zircon morphology, U -Th contents and recognition of magmatic-metamorphic growth

Much of the interpretation of age data in the present study is dependent on being able to reliably distinguish between xenocrystic, magmatic and metamorphic types of zircon. In most cases, the initial recognition of zircon type is carried out simply in terms of morphology and the assumption that a zircon rim signifies a younger overgrowth or event. The distinction between magmatic and metamorphic events is further refined with the accumulation of data and the development of a systematic pattern (see Fig. 9) which accords with geological constraints in the region. In the present study considerable assistance in the recognition of zircon type was also obtained from the correlation between zircon type and U -Th content (Fig. 4).

Zircons in rocks of the OCD are composite and heterogeneous and reflect the complex association between preservation or incorporation of xenocrystic grains, magmatic growth and metamorphic overgrowth. Figure 3, a collage of plane transmitted light microphotographs and corresponding cathodoluminescence imagery of analysed grains, shows that zircon morphology can be subdivided into (1) composite grains comprising a core and, generally, a single overgrown rim; and (2) homogeneous, largely structureless grains. Cores represent either xenocrysts or magmatic grains; the latter are often recognised in the orthogneisses of the OCD by delicate magmatic zonation which is texturally distinct from the rather homogeneous metamorphic rimming. Structureless grains are either magmatic or metamorphic, with the distinction becoming particularly unclear in rocks whose emplacement coincides with peak metamorphism. Rims are almost invariably metamorphic overgrowths and consistently record the timing of the metamorphic climax in the region. Exceptions are the zircon overgrowths observed in the Concordia and Rietberg Granites which record ages that are distinctly younger than the major period of metamorphism. It is noted that magmatic zircon growth seldom appears to nucleate around xenocrystic cores.

In the OCD the recognition of magmatic and metamorphic zircon domains is assisted by the presence of diagnostic U and Th contents. Metamorphic overgrowths are almost always characterised by higher U contents and lower Th/U ratios than corresponding magmatic or xenocrystic zircons in the same rock (Fig. 4). This is believed to be the result of selective partitioning of U (but not Th) into the metamorphic fluid associated with the wide variety of mineral reaction products, including the growth of new zircon, accompanying the granulite facies overprint. Although experimental work at high temperatures is limited, Nguyen Trung (1985) has shown that at $T=400^{\circ}\text{C}$ and $5 \leq \text{pH} \leq 9$, the $\text{UO}_2(\text{OH})_2^{\circ}$ complex is stable and could be responsible for the presence of uranium in aqueous solution. The partitioning of U into the metamorphic fluid suggests that it was sufficiently oxidising to convert tetravalent U into its labile hexavalent form, without similarly affecting Th.

In a U vs. Th plot for the Little Namaqualand Suite, the distinction between metamorphic rims on the one hand, and magmatic cores and structureless grains on the other, is clearly apparent (Fig. 4a). Although Th contents in all grains occupy the same range (50-250 ppm), the U contents of the metamorphic rims are markedly higher. In the Spektakel Suite, however, the Rietberg granite contains a population of clear structureless grains (a zircon type interpreted as magmatic in the Little Namaqualand Suite) which has U contents characteristic of metamorphic growth, distinguishing it clearly from the magmatic population in this sample (Fig. 4b). The interpretation of zircon types in terms of their U -Th contents is clearly useful and is referred to again in the sections to follow.

Fig.3: Microphotographs showing the composite morphology of zircons from various rock types in the Okiep Copper District; plane transmitted light (PT) and cathodoluminescence imagery (CL). Ages shown for individual spot analyses are $^{207}\text{Pb}/^{206}\text{Pb}$ ages from Tables 2 to 5.

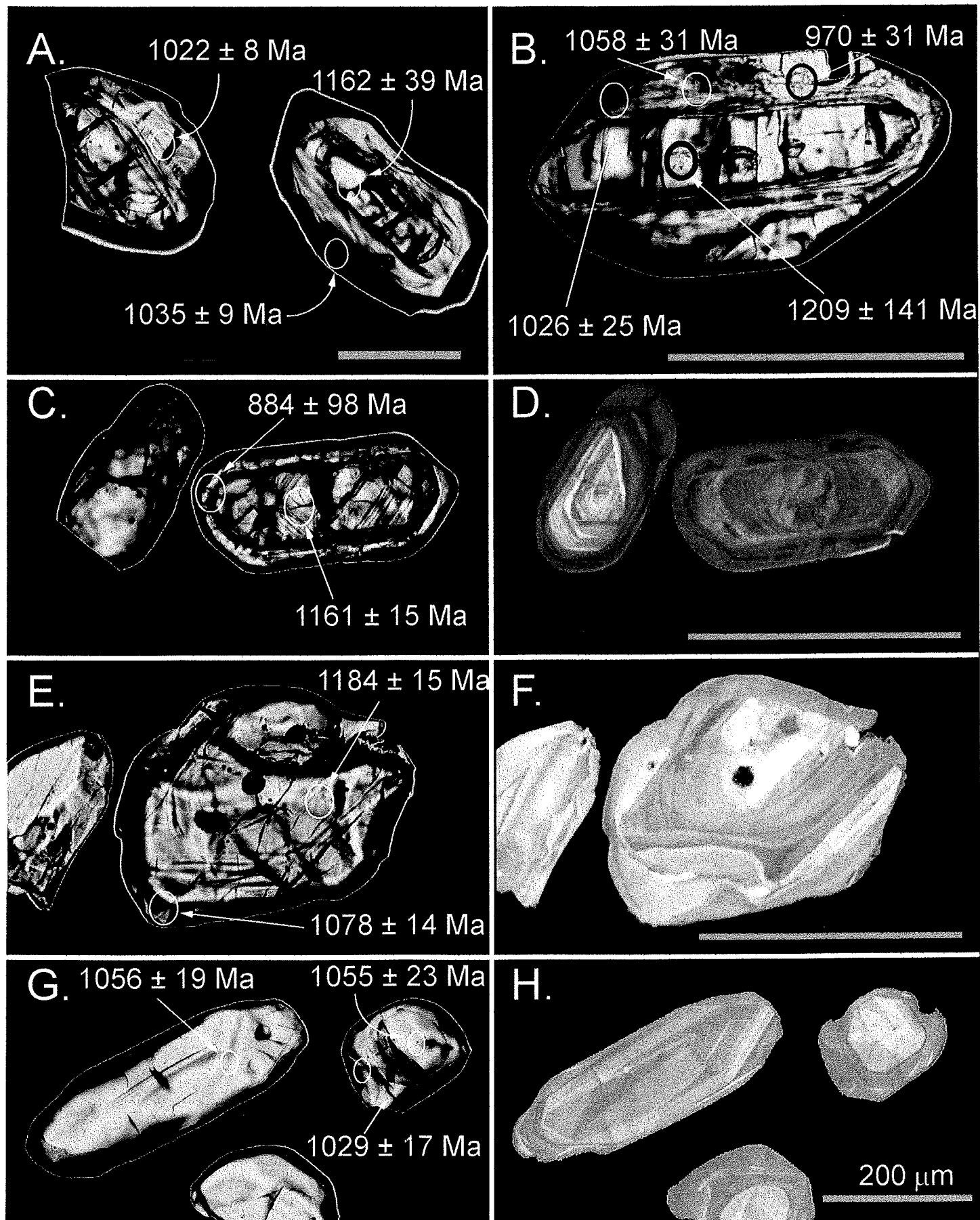
A: Zircons with distinctive cores and overgrowths from the Modderfontein gneiss (PT);

B: Zircon with distinctive core and overgrowth from anorthosite of the Koperberg Suite (PT).

C and D: Zoned zircons from the Concordia granite. Zircon overgrowths in this sample, as well as the Rietberg granite, yielded young ages of around 850 Ma. (PT and CL).

E and F: Zircons from the 2-pyroxene granulite revealing no apparent zonation in plane transmitted light; CL imagery shows a distinctive core and a complex pattern of overgrowths.

G and H: Zircons from the diorite of the Koperberg Suite. CL imagery shows the presence of structureless grains or distinctive low-U cores with pronounced overgrowths.



Note : Scale bar in all photographs is 200 microns in length

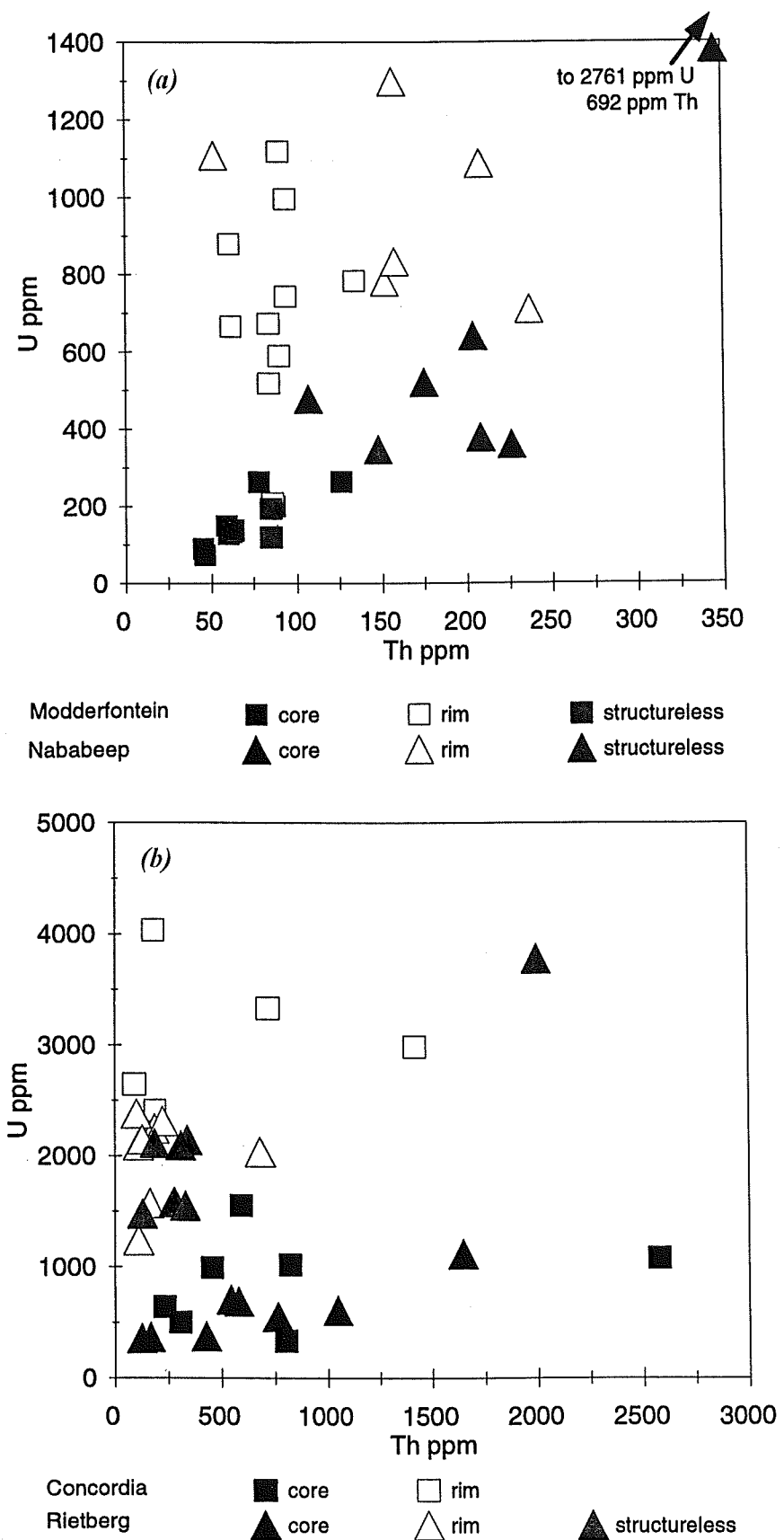


Fig. 4: Plots of U versus Th for the various zircon grains and overgrowths analysed in the present study, for (a) the Little Namaqualand Suite and (b) the Spektakel Suite.

Zircon U-Pb isotope data

Gladkop Suite (NAM6 and NAM7)

The granitic Brandewynsbank orthogneiss (NAM6) comprises two distinct types of zircon; large, brown composite grains with well-defined cores and rims and small, clear, structureless grains. The latter are considered to represent a magmatic population which yield a weighted mean $^{207}\text{Pb}/^{206}\text{Pb}$ age of **1822±36 Ma** (Fig. 5a). This is indistinguishable from the whole rock

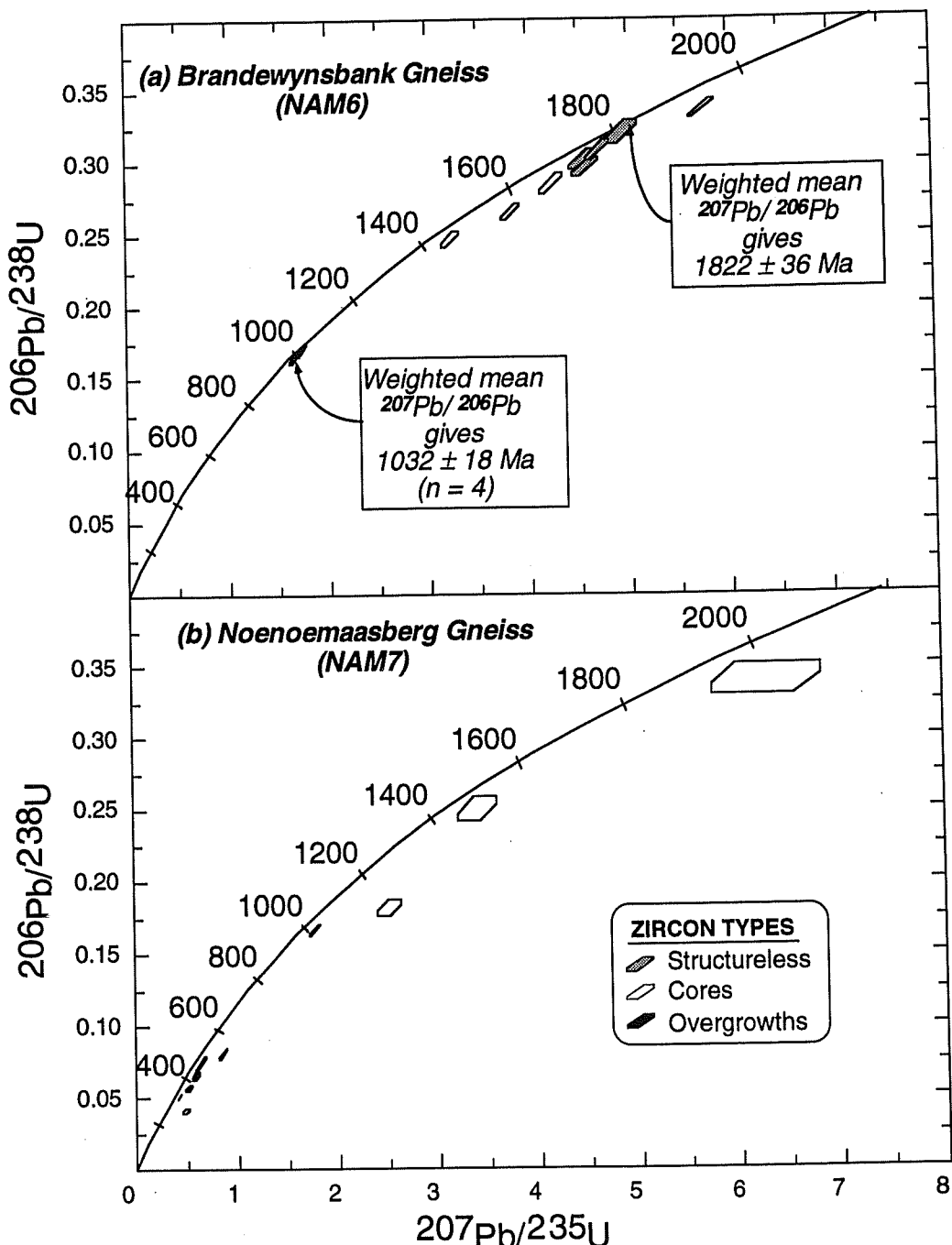


Fig. 5: $^{206}\text{Pb}/^{238}\text{U}$ versus $^{207}\text{Pb}/^{235}\text{U}$ concordia plots for zircons from (a) Brandewynsbank gneiss and (b) Noenoemaasberg gneiss of the Gladkop Suite.

Rb-Sr age of 1824 ± 70 Ma (Barton, 1983) for the suite as a whole and is considered to be the age of emplacement of the igneous precursor to the Brandewynsbank orthogneiss. Zircon cores mainly reflect the magmatic population but are discordant and have suffered Pb loss, probably during metamorphism of the suite. One core is clearly xenocrystic and has a $^{207}\text{Pb}/^{206}\text{Pb}$ age of 2018 ± 8 Ma (Table 2). The zircon rims define a tight cluster of ages with a weighted mean $^{207}\text{Pb}/^{206}\text{Pb}$ age of 1032 ± 18 Ma (Fig. 5a). This is interpreted to reflect the age of metamorphism of the suite and is the timing of the event which was responsible for the growth of new zircon around many of the existing grains.

Zircons from the leucocratic Noenoemasberg orthogneiss (NAM7), which is intimately interlayered with NAM6, are characterised by very high uranium contents and, consequently, are metamict and have discordant U-Pb isotopic ratios (Fig. 5b). Zircons are composite and, like NAM6, have well-defined cores and rims. Three of the cores are xenocrystic, but are somewhat discordant reflecting ages in the range 1600-2150 Ma (Table 2). Zircon rims are also very discordant and appear to have formed somewhere between 700-100 Ma, with recent Pb loss. Little meaningful age information is available from this sample although the available data are consistent with it having been subjected to a similar history as the Brandewynsbank gneiss, namely, emplacement at around 1800 Ma and metamorphism at about 1000 Ma.

Little Namaqualand Suite (NAM1 and NAM2) and Two-pyroxene Granulite (NAM3)

The Modderfontein orthogneiss, which intrudes the Nababeep orthogneiss in the vicinity of the Springbok dome, provides reasonably well-constrained U -Pb zircon age data. Zircons in NAM1 are typically composite with well-defined cores and rims as well as occasional clear, structureless grains. The age pattern is relatively well defined in this sample; cores and clear, structureless grains define a weighted mean $^{207}\text{Pb}/^{206}\text{Pb}$ age of 1199 ± 12 Ma, while the rims define an equally well-constrained age of 1032 ± 12 Ma (Fig. 6a). The former date is statistically indistinguishable from available whole rock Rb-Sr dates (1179 ± 28 Ma; Barton, 1983: 1223 ± 48 Ma; Clifford et al., 1994) and is interpreted to represent the age of emplacement of the magmatic protolith to the Modderfontein orthogneiss. The latter date is identical to the age of zircon rims in the Gladkop Suite and is considered to be the result of a metamorphic overprint which affected both units, causing growth of new zircon around existing grains.

Sample NAM2 of the Nababeep gneiss was collected close to the intrusive contact with the Modderfontein orthogneiss (Fig. 2). Zircons in both samples are very similar in appearance with well-defined cores and rims and some clear structureless grains. Isotopically, however, the grains exhibit a more complex age pattern, as seen in the concordia plot in Figure 6a. The analysis of a discordant zircon core (grain 6) reveals the presence of an inherited xenocrystic component with a minimum $^{207}\text{Pb}/^{206}\text{Pb}$ age of 1482 ± 18 Ma. Most of the remaining data points plot as a cluster of variably discordant analyses , with the nine most concordant analyses giving a weighted mean $^{207}\text{Pb}/^{206}\text{Pb}$ age of 1212 ± 11 Ma. This group includes clear, structureless zircon grains, as well as more complex crystals with unstructured cores grading into compositionally zoned margins. These zircons are interpreted to be magmatic in origin (see U and Th contents in Table 3 and Fig. 4a) and are considered to reflect the time of emplacement of the magmatic protolith to the Nababeep gneiss.

The zircon overgrowths in NAM2 are all variably discordant but, unlike the well constrained 1030 Ma age obtained for the Modderfontein rims, these domains exhibit a range in

Table 2: U-Th-Pb SHRIMP data for the Gladkop Suite

Grain, spot	U(ppm)	Th(ppm)	Pb(ppm)	Pb*(ppm)	204Pb/206Pb	% f206	206Pb/238U	±	207Pb/235U	±	207Pb/206Pb	±	AGES (in Ma)		
													206Pb/238U 207Pb/235U 207Pb/206Pb		
NAM6: Brandewynsbank Gneiss															
1.1s	163	328	2.01	74	0.000001	-	0.3085	0.0069	4.726	0.120	0.1111	0.0011	1733	1772	1818
2.1s	91	98	1.08	34	0.000123	0.19	0.3016	0.0074	4.575	0.135	0.1100	0.0015	1699	1745	1800
3.1s	228	412	1.81	87	0.000002	-	0.2657	0.0058	3.840	0.097	0.1048	0.0010	1519	1601	1711
4.1s	67	80	1.19	27	0.000271	0.42	0.3207	0.0085	4.964	0.170	0.1123	0.0021	1793	1836	188
5.1s	98	121	1.23	37	0.000008	0.01	0.2967	0.0071	4.609	0.131	0.1127	0.0014	1675	1751	1843
6.1r	1575	186	0.12	246	0.000544	0.92	0.1635	0.0033	1.663	0.039	0.0738	0.0007	976	994	1035
6.2c	986	425	0.43	360	0.000389	0.60	0.3366	0.0070	5.767	0.125	0.1243	0.0006	1870	1941	2018
7.1r	1230	241	0.20	205	0.000160	0.27	0.1705	0.0035	1.749	0.039	0.0744	0.0005	1015	1053	114
9.1r	1659	139	0.08	264	0.000075	0.13	0.1686	0.0034	1.709	0.037	0.0735	0.0004	1004	1012	1029
9.2c	264	169	0.64	76	0.000277	0.43	0.2468	0.0055	3.236	0.087	0.0951	0.0012	1422	1466	1530
11.1r	1710	158	0.09	265	0.000039	0.07	0.1636	0.0034	1.658	0.035	0.0735	0.0003	977	992	1028
11.2c	204	302	1.48	77	0.000070	0.11	0.2850	0.0068	4.256	0.113	0.1083	0.0010	1617	1685	1771
NAM7: Noenemaasberg Gneiss															
1.1c	43	34	0.78	12	0.000547	0.88	0.2491	0.0082	3.421	0.193	0.0996	0.0042	1434	1509	1617
1.2r	2934	165	0.06	168	0.005995	10.42	0.0569	0.0024	0.525	0.031	0.0669	0.0025	357	429	835
2.1c	175	102	0.58	39	0.001986	3.17	0.1812	0.0055	2.533	0.118	0.1014	0.0033	1073	1282	1650
2.2r	1802	104	0.06	144	0.000918	1.55	0.0808	0.0036	0.861	0.041	0.0772	0.0010	501	630	1127
3.1s	1630	70	0.04	254	0.00090	0.15	0.1663	0.0042	1.781	0.048	0.0777	0.0005	992	1039	1139
4.1c	103	153	1.49	49	0.000002	0.00	0.3395	0.0106	6.316	0.544	0.1349	0.0103	1884	2021	2163
4.2r	3337	159	0.05	227	0.000446	0.79	0.0729	0.0056	0.635	0.053	0.0632	0.0014	454	499	713
5.1r	3800	268	0.07	235	0.005357	9.35	0.0647	0.0029	0.586	0.040	0.0657	0.0032	404	468	796
6.1c	2536	111	0.04	121	0.000478	0.85	0.0507	0.0016	0.423	0.015	0.0606	0.0007	319	359	626
7.1c	758	130	0.17	35	0.001933	3.17	0.0404	0.0016	0.489	0.030	0.0879	0.0037	255	404	1379
7.2r	2652	161	0.06	176	0.002092	3.54	0.0648	0.0030	0.673	0.040	0.0754	0.0023	404	522	1078

Notes:

(1) Uncertainties are at the one sigma level

(2) - signifies no 204Pb detected

(3) %f206 = common 206Pb as a percentage of total 206Pb

(4) * = radiogenic Pb

(5) Zircon types: c = core; r = overgrowth; s = homogenous, structureless grain.

(6) %Conc = percentage concordancy

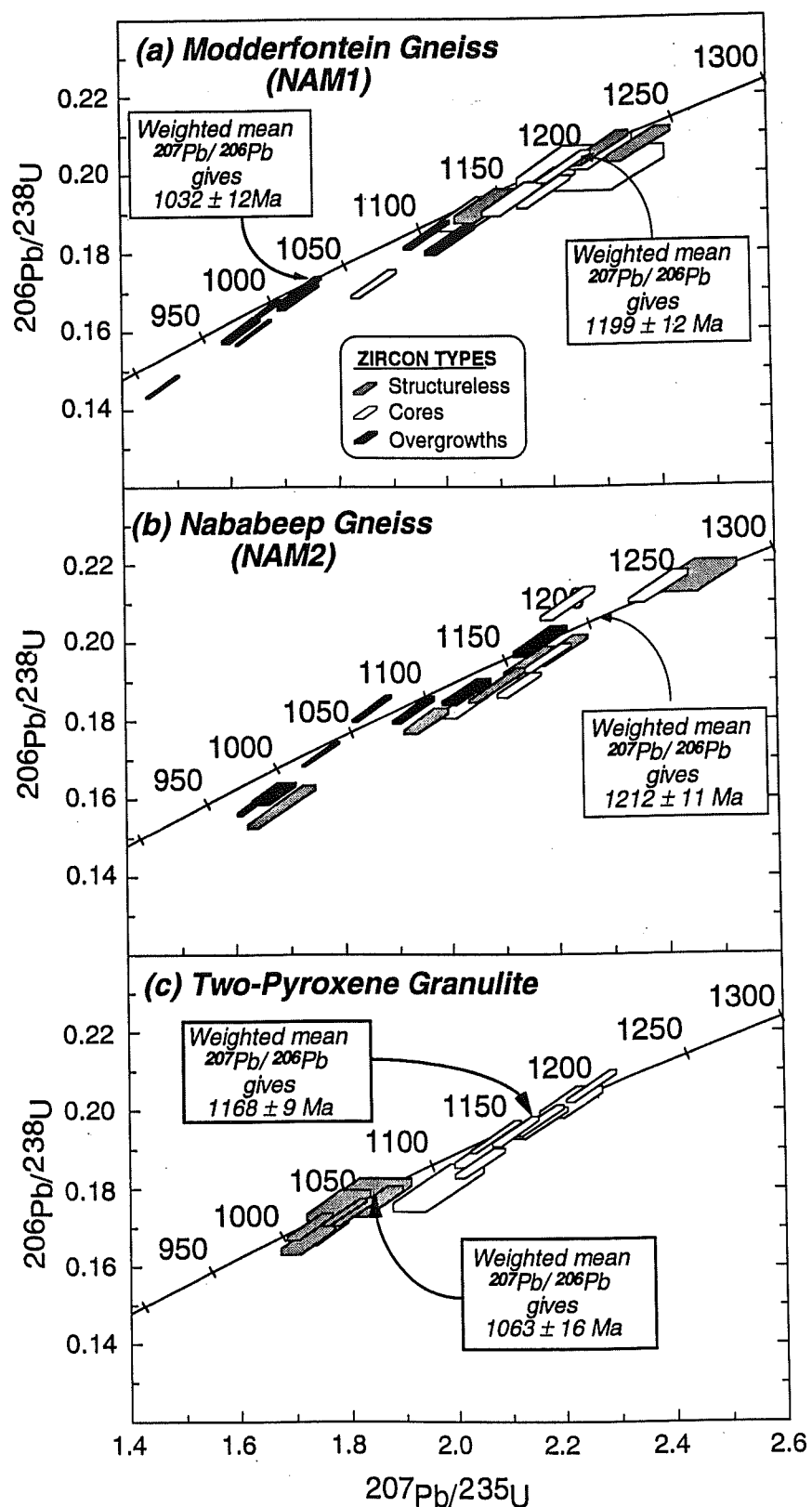


Fig 6: $^{206}\text{Pb}/^{238}\text{U}$ versus $^{207}\text{Pb}/^{235}\text{U}$ concordia plots for zircons from (a) Nababeep gneiss (b) Modderfontein gneiss and (c) two-pyroxene granulite of the Little Namaqualand Suite.

Table 3: U-Th-Pb SHRIMP data for the Little Namaqualand Suite

	Grain:spot	U(ppm)	Th(ppm)	Th/U	Pb*(ppm)	204Pb/206Pb	% f206	206Pb/238U	±	207Pb/235U	±	207Pb/206Pb	±	AGES (in Ma)			
														206Pb/238U	207Pb/235U	207Pb/206Pb	±
NAM1: Modderfontein Gneiss																	
1.1c	74	46	0.62	16	0.000245	0.40	0.2011	0.0059	2.275	0.136	0.0821	0.0040	1181	1205	1247	99	95
1.2r	881	61	0.07	141	0.000056	0.09	0.1702	0.0035	1.731	0.037	0.0738	0.0003	1013	1020	1035	9	98
2.1c	264	78	0.29	52	0.000049	0.08	0.1951	0.0041	2.189	0.051	0.0814	0.0006	1149	1178	1230	14	93
2.2r	745	94	0.13	130	0.000053	0.09	0.1843	0.0038	1.969	0.043	0.0775	0.0004	1091	1105	1134	11	96
3.1s	121	85	0.70	28	0.000031	0.05	0.2072	0.0045	2.366	0.057	0.0828	0.0007	1214	1233	1265	17	96
4.1c	149	59	0.39	32	0.000082	0.14	0.2052	0.0045	2.297	0.059	0.0812	0.0009	1203	1211	1226	22	98
4.2r	1120	90	0.08	154	0.000004	0.01	0.1459	0.0030	1.475	0.031	0.0733	0.0002	878	920	1022	6	86
5.1s	195	85	0.44	42	0.000037	0.06	0.2061	0.0044	2.293	0.054	0.0807	0.0006	1208	1210	1214	14	100
6.1c	129	60	0.46	26	0.000126	0.21	0.1934	0.0043	2.130	0.056	0.0759	0.0009	1140	1159	1193	22	96
6.2r	785	134	0.17	126	0.000082	0.14	0.1687	0.0035	1.729	0.038	0.0743	0.0005	1005	1020	1051	12	96
7.1c	265	126	0.48	56	0.000057	0.09	0.2014	0.0042	2.228	0.051	0.0802	0.0005	1183	1190	1202	13	98
7.2r	667	62	0.09	101	0.000011	0.02	0.1597	0.0033	1.646	0.035	0.0747	0.0002	955	988	1062	6	90
8.1c	91	45	0.49	18	0.000225	0.38	0.1898	0.0044	2.057	0.065	0.0786	0.0015	1120	1134	1162	39	96
8.2r	675	84	0.12	110	0.000024	0.04	0.1705	0.0035	1.734	0.037	0.0758	0.0003	1015	1021	1035	9	98
9.1r	591	90	0.15	93	0.000031	0.05	0.1646	0.0034	1.663	0.035	0.0733	0.0003	982	994	1022	8	96
10.1s	135	62	0.46	27	0.000099	0.17	0.1917	0.0043	2.079	0.057	0.0787	0.0011	1131	1142	1163	27	97
11.1c	138	63	0.46	28	0.000105	0.18	0.1970	0.0043	2.192	0.058	0.0807	0.0011	1159	1178	1214	26	96
11.2r	209	86	0.41	40	0.0000131	0.22	0.1831	0.0038	2.013	0.047	0.0797	0.0007	1084	1120	1190	16	91
12.1r	997	94	0.09	122	0.000083	0.14	0.1290	0.0026	1.292	0.028	0.0726	0.0004	782	842	1004	10	78
13.1r	520	84	0.16	80	0.000057	0.10	0.1604	0.0033	1.622	0.036	0.0734	0.0005	959	979	1024	14	94
14.1c	201	87	0.43	36	0.000022	0.04	0.1720	0.0037	1.869	0.043	0.0788	0.0005	1023	1070	1168	13	88
NAM2: Nababeep Gneiss																	
1.1s	378	208	0.55	80	0.000040	0.07	0.1976	0.0041	2.207	0.051	0.0810	0.0007	1163	1183	1222	17	95
2.1c	479	107	0.22	99	0.000046	0.08	0.2096	0.0043	2.223	0.050	0.0769	0.0006	1227	1188	1119	15	110
2.2r	1299	157	0.12	227	0.000003	-	0.1829	0.0035	1.853	0.037	0.0735	0.0004	1083	1064	1027	10	105
3.1s	348	148	0.42	78	0.000078	0.14	0.2165	0.0043	2.459	0.074	0.0824	0.0017	1263	1260	1254	40	101
4.1r	782	152	0.19	144	0.000230	0.41	0.1872	0.0036	2.032	0.046	0.0787	0.0008	1106	1126	1166	20	95
4.2c	641	204	0.32	103	0.000242	0.43	0.1577	0.0055	1.686	0.063	0.0775	0.0008	944	1003	1135	19	83
5.1r	1087	208	0.19	193	0.000034	0.06	0.1824	0.0035	1.932	0.040	0.0768	0.0005	1080	1092	1117	12	97
5.2c	360	226	0.63	84	0.000097	0.17	0.2138	0.0042	2.388	0.054	0.0810	0.0007	1249	1239	1222	17	102
6.1r	833	158	0.19	139	0.000032	0.06	0.1711	0.0032	1.758	0.034	0.0745	0.0002	1018	1030	1055	6	97
6.2c	521	175	0.34	131	0.000026	0.05	0.2399	0.0065	3.067	0.091	0.0927	0.0009	1386	1424	1482	18	94
7.1r	1109	52	0.05	208	0.000058	0.10	0.2001	0.0040	2.171	0.051	0.0787	0.0008	1176	1172	1164	21	101
7.2c	710	237	0.33	140	0.000098	0.18	0.1947	0.0039	2.151	0.048	0.0801	0.0006	1165	1200	1220	16	96
7.3c	2761	692	0.25	300	0.000142	0.25	0.1043	0.0024	1.003	0.025	0.0698	0.0005	640	705	921	15	69

Table 3: cont.

	Grain/spot	U(ppm)	Th(ppm)	Pb*(ppm)	204Pb/206Pb	% f206	206Pb/238U	±	207Pb/235U	±	207Pb/206Pb	±	206Pb/238U	±	207Pb/235U	±	207Pb/206Pb	±	AGES (in Ma)	
NAM2: Nababeep Gneiss (cont.)																				
8.1s	709	147	0.21	125	0.000122	0.21	0.1796	0.0033	1.956	0.043	0.0790	0.0008	1065	1100	1171	19	91			
10.1s	1091	328	0.30	208	0.000067	0.11	0.1887	0.0045	2.089	0.053	0.0803	0.0005	1114	1145	1204	12	93			
11.1c	474	123	0.26	92	0.000001	-	0.1957	0.0038	2.181	0.046	0.0808	0.0005	1152	1175	1218	13	95			
12.1c	764	398	0.52	154	0.000081	0.14	0.1889	0.0032	2.130	0.041	0.0818	0.0006	1116	1159	1240	14	90			
13.1r	905	108	0.12	137	0.000001	-	0.1585	0.0028	1.636	0.030	0.0749	0.0004	948	984	1064	10	89			
15.1r	752	154	0.20	119	0.000112	0.19	0.1612	0.0029	1.673	0.040	0.0753	0.0010	963	998	1076	27	90			
16.1c	666	151	0.23	121	0.000132	0.22	0.1839	0.0034	2.027	0.046	0.0800	0.0009	1088	1125	1196	21	91			
NAM3: Two-pyroxene Granulite																				
1.1s	77	43	0.56	14	0.000286	0.48	0.1693	0.0038	1.743	0.055	0.0747	0.0015	1008	1025	1061	40	95			
1.2s	173	139	0.80	37	0.000057	0.10	0.1894	0.0040	2.047	0.049	0.0784	0.0007	1118	1131	1156	18	97			
2.1s	136	140	1.03	29	0.000060	0.10	0.1767	0.0039	1.851	0.048	0.0760	0.0008	1049	1064	1094	22	96			
3.1c	339	140	0.41	65	0.000010	0.02	0.1886	0.0039	2.044	0.047	0.0795	0.0006	1103	1130	1184	15	93			
3.2r	188	39	0.21	32	0.000019	0.03	0.1740	0.0037	1.808	0.041	0.0753	0.0005	1034	1048	1078	14	96			
4.1s	98	58	0.60	18	0.000182	0.31	0.1668	0.0037	1.723	0.048	0.0750	0.0011	994	1017	1067	30	93			
5.1s	414	104	0.25	70	0.000065	0.11	0.1703	0.0035	1.729	0.041	0.0736	0.0006	1014	1019	1032	17	98			
5.2s	212	62	0.29	37	0.000006	0.01	0.1738	0.0037	1.791	0.040	0.0747	0.0004	1033	1042	1061	11	97			
6.1s	157	74	0.47	33	0.000149	0.25	0.2021	0.0040	2.215	0.057	0.0795	0.0011	1187	1186	1185	28	100			
6.2s	508	228	0.45	104	0.000055	0.09	0.1967	0.0041	2.160	0.049	0.0796	0.0006	1157	1168	1188	14	97			
6.3s	67	45	0.68	13	0.001093	1.84	0.1793	0.0035	1.842	0.072	0.0745	0.0024	1063	1061	1056	65	101			
7.1s	95	53	0.56	18	0.000001	0.00	0.1802	0.0062	1.966	0.086	0.0791	0.0018	1068	1104	1176	46	91			
8.1s	355	435	1.23	87	0.000018	0.03	0.1974	0.0040	2.157	0.047	0.0793	0.0005	1161	1167	1178	12	99			
9.1s	91	54	0.59	17	0.000067	0.11	0.1757	0.0040	1.780	0.058	0.0735	0.0015	1043	1038	1028	42	102			
10.1s	686	977	1.42	171	0.000017	0.03	0.1932	0.0042	2.075	0.046	0.0779	0.0003	1139	1141	1144	8	100			
11.1s	465	259	0.56	97	0.000001	0.00	0.1945	0.0037	2.112	0.044	0.0788	0.0005	1146	1153	1167	11	98			
12.1s	452	545	1.21	115	0.000013	0.02	0.2059	0.0040	2.254	0.046	0.0794	0.0004	1207	1198	1181	9	102			

Notes:
(1) Uncertainties are at the one sigma level
(2) - signifies no 204Pb detected
(3) %f206 = common 206Pb as a percentage of total 206Pb
(4) * = radiogenic Pb

(5) Zircon types: c = core; r = overgrowth; s = homogenous, structureless grain.
(6) %Conc = percentage concordancy

$^{207}\text{Pb}/^{206}\text{Pb}$ ages (Table 3). At least 4 of the overgrowths could have formed at around 1030-1060 Ma and reflect growth in response to the same metamorphic event that is so clearly recorded in the intrusive Modderfontein gneiss and older Gladkop Suite. Other overgrowths must, however, be older and appear to have grown at around 1165 Ma (analyses 4.1 and 7.1). These overgrowths are, therefore, interpreted as the product of polymetamorphic growth, either in response to local (contact?) metamorphism of the NAM2 sample (Nababeep gneiss) by intrusion of the nearby Modderfontein gneiss at 1200 Ma, or the regional metamorphism at 1060 - 1030 Ma. The age patterns of all the zircons and zircon domains in the Nababeep gneiss are further complicated by the effects of multi-stage Pb loss.

The two-pyroxene granulite is an enigmatic unit of mafic to intermediate composition which occurs as layers and elongate lenses over a large area of the NMC, but in the OCD mainly to the east of the Springbok antiform. It was originally assigned to the Lammerhoek Subgroup (not recognised by SACS, 1980) and thought to occur as xenoliths, mainly in the Nababeep orthogneiss. It has also been interpreted as a metamorphosed mafic sill (Lombaard et al., 1986) intruding the Nababeep gneiss. Zircons in this unit are very unusual with respect to most of the other rocks of the NMC and are typically subhedral with no well-defined core-rim texture. Although most of the zircons are apparently homogeneous in appearance they define two well-constrained age populations, although, more often than not, these isotopic domains are not texturally identifiable in terms of a core-rim arrangement. The older zircon domains have a weighted mean $^{207}\text{Pb}/^{206}\text{Pb}$ age of **1168±9 Ma** while the younger domain exhibits an age of **1063±16 Ma** (Fig. 6c). The former date is similar to a multiple zircon population U -Pb concordia age of 1160 ± 50 Ma (Clifford et al., 1981) and is interpreted as the age of emplacement of the two-pyroxene granulite. This indicates that, at least at the locality sampled in the present study, this unit was intruded as a sill into the ca. 1220 Ma old Nababeep gneiss. The 1063 Ma date is regarded as a metamorphic overprint which resulted in poorly structured growth and overgrowth of zircon.

Spektakel Suite (NAM4 and NAM8)

Zircons in the Concordia granite (NAM4) are generally small, cracked, and often metamict due to high U and Th contents (Table 4). Most grains are composite and have well-defined cores and rims. One of the cores analysed (grain 1.1, Fig. 7a) is probably xenocrystic and has a $^{207}\text{Pb}/^{206}\text{Pb}$ age of 1161 ± 15 Ma. The remaining cores commonly exhibit a primary growth banding (Fig. 3) and are regarded as a magmatic population, a feature which is also confirmed in terms of their U and Th contents relative to metamorphosed rims (Fig. 4b). The magmatic cores yield a weighted mean $^{207}\text{Pb}/^{206}\text{Pb}$ age of **1064±31 Ma**, which is regarded as the emplacement age of the granite and is somewhat younger than the previously published whole rock Rb-Sr errorchron age of 1105 ± 24 Ma (Clifford et al., 1994). Zircon rims are discordant because of metamictisation and recent lead loss, but nevertheless provide a relatively imprecise age of **861±45 Ma**. This age is distinctly different from the age of zircon rims which define the regional metamorphic overprint (at 1060-1030 Ma) in the previous samples. As discussed in more detail later, it appears that the emplacement of the Concordia granite was coeval with the onset of granulite facies metamorphism in the region, such that a clear distinction between pre-granulite cores and syn-granulite rims is not apparent. The Concordia zircons nevertheless record the formation of overgrowths onto existing grains during an event, whose significance is largely under-emphasised in the NMC, at ca. 860 Ma. This age is also reflected in K -Ar and Ar-Ar whole rock ages of 800-850 Ma (Clifford et al., 1994) and has been attributed to cooling plateaux in these isotope systems. Such an explanation does not, however, accord with the

growth of zircon rims at this time and the latter may rather reflect the initiation of a new orogenic episode at ca. 850 Ma (see later).

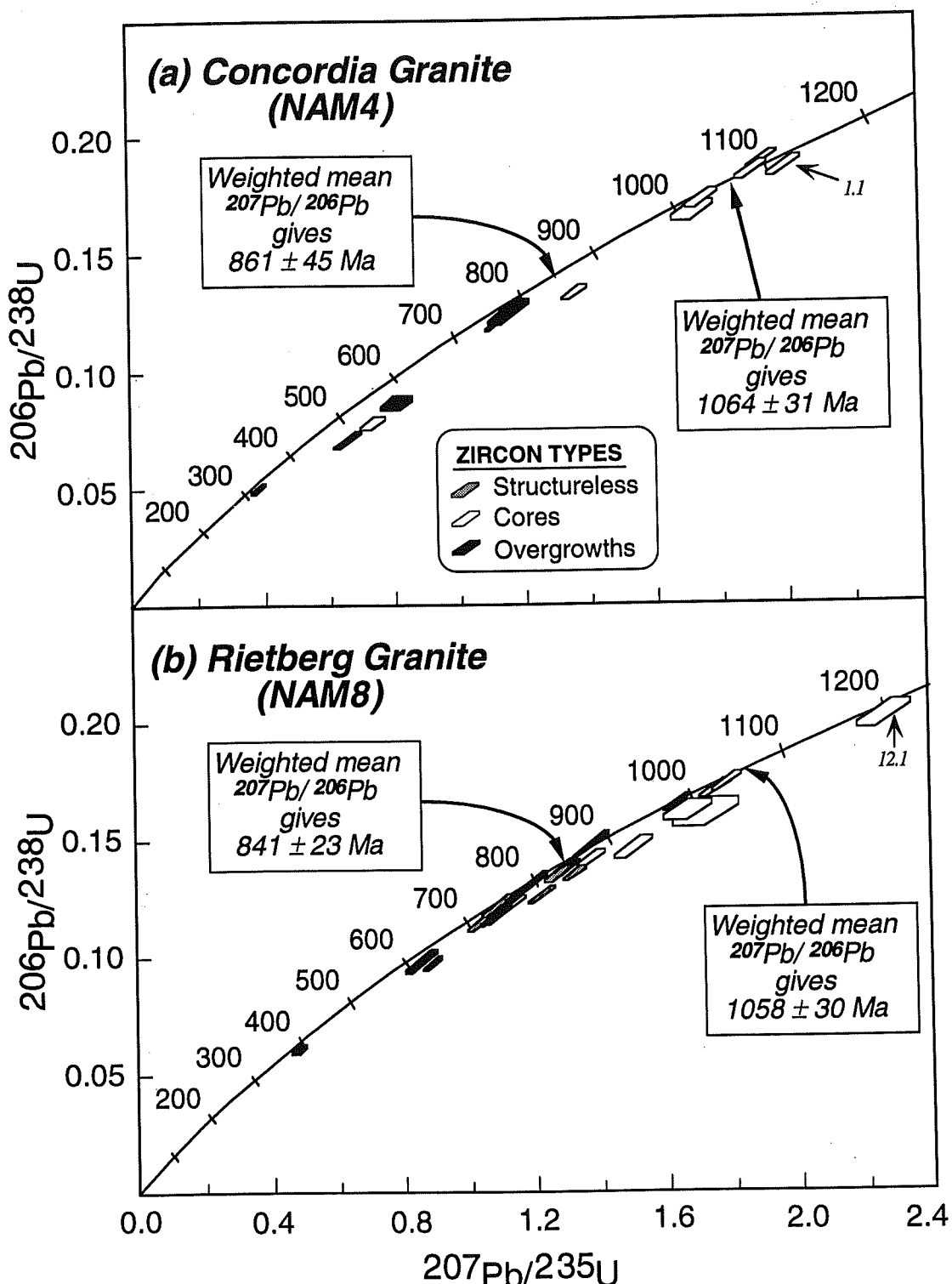


Fig 7: $^{206}\text{Pb}/^{238}\text{U}$ versus $^{207}\text{Pb}/^{235}\text{U}$ concordia plots for zircons from (a) Concordia granite and (b) Rietberg granite of the Spektakel Suite.

Table 4: U-Th-Pb SHRIMP data for the Spektakel Suite

Grain spot	U(ppm)	Th(ppm)	Th/U	Pb*(ppm)	204Pb/206Pb	% 1206	AGES (in Ma)		
							206Pb/238U	207Pb/235U	207Pb/206Pb
NAM 4: Concordia Granite									
1.1c	995	456	0.46	194	0.000373	0.63	0.1857	0.0043	2.011
1.2r	2410	187	0.08	202	0.007312	12.41	0.0862	0.0031	0.815
2.1c	502	305	0.61	92	0.000997	1.69	0.1669	0.0044	1.732
3.1r	4036	180	0.04	278	0.002604	4.42	0.0705	0.0041	0.662
4.1c	643	231	0.36	89	0.000245	0.42	0.1329	0.0031	1.363
4.2r	2647	89	0.03	301	0.000145	0.25	0.1225	0.0058	0.074
5.1c	1553	595	0.38	130	0.001277	2.17	0.0776	0.0029	0.741
5.2r	3332	723	0.22	170	0.001595	2.71	0.0495	0.0025	0.386
6.1r	2989	1421	0.48	387	0.005456	9.26	0.1247	0.0056	1.161
7.1c	337	803	2.39	94	0.000026	0.04	0.1842	0.0042	1.913
8.1c	1022	822	0.80	202	0.000679	1.15	0.1724	0.0042	1.762
10.1c	1083	2576	2.38	285	0.000280	0.48	0.1886	0.0041	1.944
NAM 8: Rietberg Granite									
1.1c	610	1049	1.72	126	0.000421	0.72	0.1459	0.0048	1.504
1.2r	1571	160	0.10	245	0.000120	0.21	0.1649	0.0040	1.636
2.1c	1117	1647	1.47	213	0.000194	0.33	0.1413	0.0037	1.373
2.2r	2246	186	0.08	206	0.000209	0.36	0.0969	0.0028	0.891
3.1s	1582	278	0.18	215	0.000778	1.23	0.1349	0.0036	1.274
4.1c	357	123	0.35	61	0.001225	2.09	0.1605	0.0061	1.722
4.3r	2312	225	0.10	213	0.000521	0.89	0.0975	0.0051	0.855
5.1c	707	547	0.77	137	0.000022	0.04	0.1735	0.0040	1.784
6.1c	375	428	1.14	76	0.000458	0.78	0.1615	0.0047	1.668
6.2r	2377	99	0.04	287	0.000420	0.72	0.1294	0.0068	1.180
7.1s	1546	330	0.21	201	0.000329	0.56	0.1348	0.0032	1.324
8.1s	2116	185	0.09	227	0.000426	0.73	0.1142	0.0039	1.035
9.1s	2141	340	0.16	257	0.000137	0.23	0.1260	0.0041	1.222
10.1c	690	582	0.84	135	0.000075	0.13	0.1707	0.0043	1.752
10.2r	2093	108	0.05	230	0.000131	0.22	0.1177	0.0051	1.084
11.1s	2093	310	0.15	243	0.000552	0.94	0.1213	0.0050	1.088
12.1c	367	164	0.45	77	0.000067	0.11	0.2019	0.0059	2.263
12.2r	2147	126	0.06	276	0.000274	0.47	0.1376	0.0036	1.300
13.1s	1476	127	0.09	167	0.000217	0.37	0.1195	0.0065	1.115
14.1r	3781	1999	0.53	245	0.000748	1.28	0.0603	0.0021	0.480
14.2r	2036	685	0.34	295	0.000196	0.34	0.1470	0.0056	1.375

Notes:

(1) Uncertainties are at the one sigma level

(2) - signifies no 204Pb detected

(3) %1206 = common 206Pb as a percentage of total 206Pb

(4) * = radiogenic Pb

(5) Zircon types: c = core; r = overgrowth; s = homogenous, structureless grain.

(6) %Conc = percentage concordancy

Zircons in the Rietberg granite (NAM8) are texturally and compositionally similar, but of even poorer quality, than those from the Concordia granite. Cores and rims exhibit similar age patterns to those in the Concordia granite. One core (grain 12.1, Fig. 7b) is clearly xenocrystic and has a $^{207}\text{Pb}/^{206}\text{Pb}$ age of about 1229 ± 34 Ma. The remaining cores are interpreted as magmatic and they yield a weighted mean $^{207}\text{Pb}/^{206}\text{Pb}$ age of **1058 ± 30 Ma**, which is statistically indistinguishable from the Concordia age, but is consistent with the observations that the two granites are genetically related with the Rietberg intruding the Concordia. Rims are also interpreted similarly to those in the Concordia granite and provide a young, post-Namaquan age of **841 ± 23 Ma**. In addition, the Rietberg granite contains a few small, clear, structureless zircons with variable discordant ages falling in the range 800-950 Ma. These grains have higher U contents than the magmatic cores (Fig. 4b) and are probably indistinguishable from the rims, and most likely represent zircon growth during the 850 Ma event.

Koperberg Suite (NAM9, NAM10 and NAM11)

The various rock units of the Koperberg Suite sampled for the present study form part of a sequence that intrudes the Concordia granite (Fig. 2; Van Zweiten et al., 1996) and should, therefore, all be younger than 1064 Ma. Anorthosite sample NAM9 occurs as a large xenolith within diorite and hypersthene of the Koperberg Suite. Zircons from this sample are mostly composite grains with well-defined cores and rims and a few clear structureless grains (Fig. 3). One of the zircon cores analysed is clearly xenocrystic with a $^{207}\text{Pb}/^{206}\text{Pb}$ age of 1732 ± 17 Ma (Table 5). Most of the other cores, together with a single analysis of a structureless grain, combine to give a weighted mean $^{207}\text{Pb}/^{206}\text{Pb}$ age of **1202 ± 25 Ma** (Fig. 8a). Defining an age for the zircon overgrowths in this sample is problematical as the analyses are generally discordant (correlating with high U concentrations) and in some cases have substantial common Pb contents. An imprecise age of **1037 ± 86 Ma** can be calculated from the three near concordant analyses (3.3, 5.2 and 9.2). The age of the overgrowths is also interpreted as reflecting the timing of the regional metamorphic overprint. These data, although less precise, agree with the U - Pb zircon data published by Clifford et al. (1995) for andesine anorthosite intruding the Nababeep gneiss.

Zircons in the Koperberg Suite diorite (NAM10), which intrudes the anorthosite, are generally structureless, brown, sub- to euhedral grains of excellent quality and clarity. A smaller population of composite grains of similar habit, but with well defined cores and rims, also occurs. Statistically the isotopic ratios from the three zircon domains are indistinguishable (i.e. structureless grains **1061 ± 20 Ma**, cores **1053 ± 20 Ma** and overgrowths **1056 ± 11 Ma**) and collectively the entire population in the NAM10 diorite yields a weighted mean $^{207}\text{Pb}/^{206}\text{Pb}$ age of **1057 ± 8 Ma** (Fig. 8b). In contrast to the data for zircon overgrowths in some of the other OCD samples (e.g. NAM1, NAM6 and NAM11), the overgrowths analysed from this diorite sample do not have the distinctive low Th/U ratios recognised in overgrowths of metamorphic origin and would appear to have formed during the same magmatic/thermal event as the cores and unstructured grains.

A tentative interpretation of the diorite data is that emplacement at **1057 ± 8 Ma** accompanied the onset of regional metamorphism, which peaked at around 1030 Ma. Early Pb loss (as a consequence of the regional metamorphic peak) caused some scatter in the $^{207}\text{Pb}/^{206}\text{Pb}$ ratios, possibly blurring the geochronological distinction between the two events. Alternatively the two events discussed here may be statistical artefacts and in reality magmatism

and metamorphism might have been entirely coeval in the time span between 1060 and 1030 Ma.

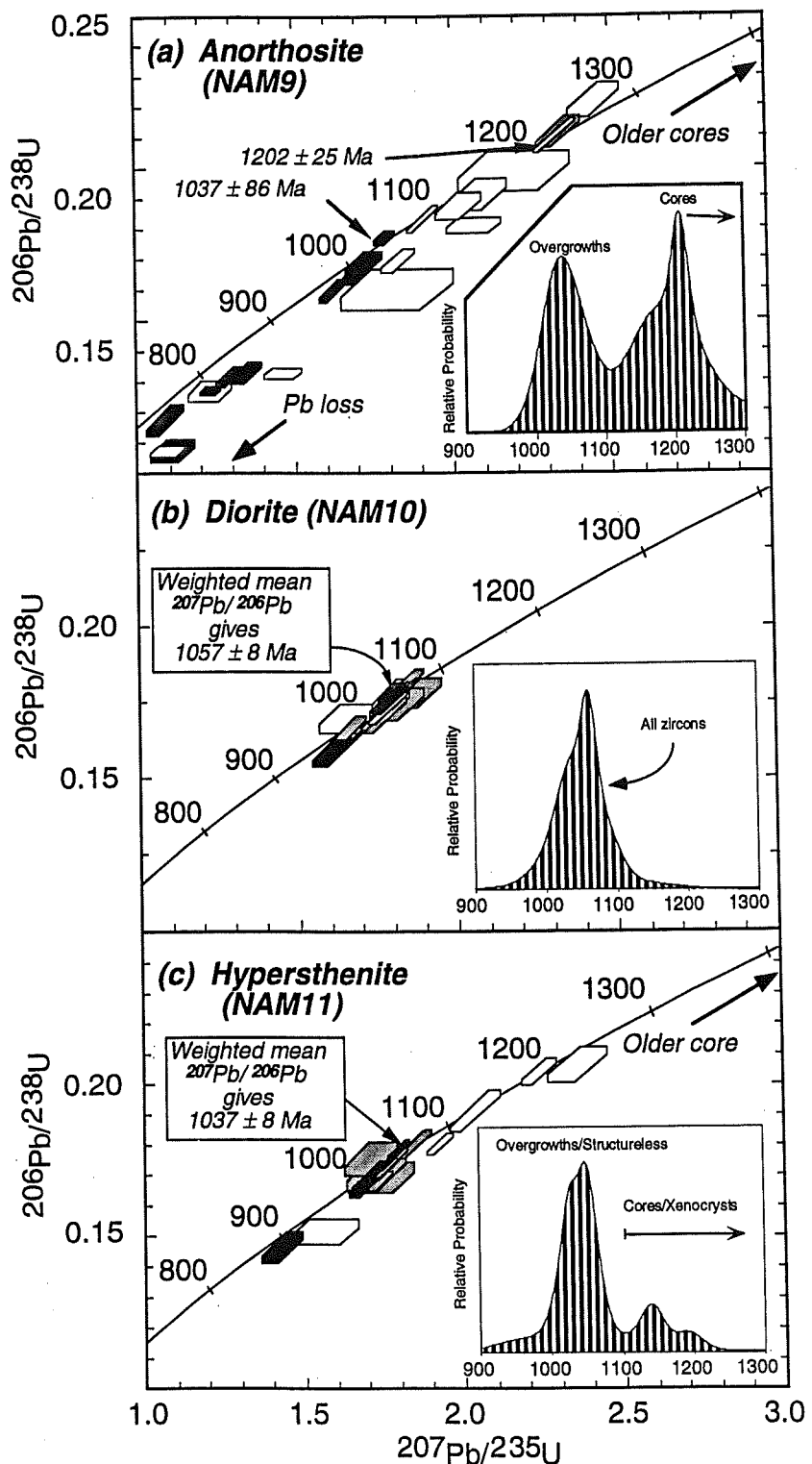


Fig 8: $^{206}\text{Pb}/^{238}\text{U}$ versus $^{207}\text{Pb}/^{235}\text{U}$ concordia plots for zircons from (a) anorthosite (b) diorite and (c) hypersthene of the Koperberg Suite. Data are plotted according to the type (core, overgrowths, structureless) as for the other concordia plots.

Table 5: U-Th-Pb SHRIMP data for the Koperberg Suite

	Grain-spot	U(ppm)	Th(ppm)	Pb ^y (ppm)	204Pb/206Pb	% f206	206Pb/238U	±	207Pb/235U	±	207Pb/206Pb	±	AGES (in Ma)		
													206Pb/238U	207Pb/235U	207Pb/206Pb
NAM9: Anorthosite															
1.1c	945	302	0.32	160	0.001393	2.351	0.1695	0.0039	1.833	0.052	0.0784	0.0011	1009	1057	1158
1.2r	2779	290	0.10	167	0.013313	22.597	0.0533	0.0027	0.454	0.043	0.0617	0.0045	335	380	664
2.1c	968	374	0.39	197	0.002163	3.610	0.1911	0.0050	2.091	0.088	0.0794	0.0024	1127	1146	1182
2.2r	3761	361	0.10	429	0.003405	5.779	0.1173	0.0051	1.086	0.057	0.0672	0.0017	715	747	843
3.2r	2041	163	0.08	263	0.002247	3.792	0.1315	0.0036	1.296	0.042	0.0714	0.0011	797	844	954
3.3r	522	212	0.41	88	0.000293	0.343	0.1659	0.0041	1.706	0.052	0.0746	0.0011	989	1011	1058
3.4c	34	46	1.36	9	0.001034	1.725	0.1986	0.0065	2.204	0.175	0.0805	0.0055	1168	1182	1209
3.5r	591	265	0.45	106	0.000361	0.615	0.1770	0.0023	1.792	0.034	0.0734	0.0009	1050	1042	1066
4.1c	769	256	0.33	164	0.000013	0.022	0.2102	0.0058	2.333	0.068	0.0805	0.0005	1230	1223	1209
4.2r	1925	330	0.17	203	0.013976	23.852	0.0904	0.0039	0.853	0.104	0.0684	0.0074	558	626	880
5.1c	410	336	0.82	86	0.000161	0.272	0.1832	0.0044	1.911	0.049	0.0757	0.0005	1084	1085	1086
5.2r	826	146	0.18	138	0.001141	1.926	0.1686	0.0040	1.726	0.060	0.0743	0.0017	1004	1018	1048
6.1c	365	173	0.47	85	0.000189	0.322	0.2220	0.0056	2.460	0.082	0.0804	0.0015	1292	1260	1206
6.2r	2240	133	0.06	289	0.002120	3.618	0.1325	0.0035	1.347	0.049	0.0737	0.0016	866	1035	44
7.1c	429	180	0.42	94	0.000296	0.505	0.2113	0.0052	2.346	0.071	0.0805	0.0012	1236	1226	1210
7.1s									1.233	0.071	0.0706	0.0034	768	816	946
8.1c	1034	530	0.51	135	0.003068	5.236	0.1266	0.0032	1.110	0.072	0.0752	0.0038	655	758	1074
8.2r	2152	329	0.15	267	0.008527	14.552	0.1070	0.0038	4.379	0.122	0.1060	0.0010	1689	1708	1732
9.1c	330	137	0.42	105	0.000183	0.312	0.2996	0.0076	0.246	0.071	0.0805	0.0012	1236	1226	1210
9.2r	1214	220	0.18	192	0.000928	1.567	0.1597	0.0037	1.623	0.044	0.0737	0.0009	955	979	1034
10.1c	612	536	0.88	138	0.001611	2.719	0.1872	0.0044	2.026	0.074	0.0785	0.0020	1106	1124	1159
10.2r	4215	748	0.18	405	0.021400	36.522	0.0509	0.0031	0.625	0.072	0.0890	0.0080	320	493	1403
11.1c	470	266	0.57	172	0.000231	0.357	0.3335	0.0045	5.215	0.133	0.1134	0.0023	1855	1855	36
11.2r	2450	123	0.05	245	0.002432	4.132	0.1047	0.0012	0.985	0.022	0.0882	0.0012	642	696	875
12.1r	3176	125	0.04	394	0.003935	6.686	0.1267	0.0015	1.234	0.033	0.0706	0.0016	769	816	946
13.1c	1529	531	0.35	186	0.004203	7.140	0.1071	0.0019	1.092	0.051	0.0740	0.0031	656	750	1041
14.1r	803	161	0.20	133	0.000636	1.080	0.1689	0.0021	1.728	0.034	0.0742	0.0011	1006	1019	1046
14.2c	310	165	0.53	48	0.002791	4.712	0.1324	0.0018	1.464	0.058	0.0802	0.0029	802	916	1201
15.1c	364	221	0.61	73	0.005057	8.374	0.1601	0.0067	1.829	0.179	0.0829	0.0059	957	1056	1267
15.2c	536	421	0.78	121	0.003580	5.926	0.1808	0.0026	2.075	0.085	0.0832	0.0030	1071	1140	1275
15.3r	2364	173	0.07	221	0.004401	7.477	0.0960	0.0012	0.852	0.027	0.0543	0.0018	591	626	753
16.1r	4538	202	0.04	232	0.014083	23.930	0.0443	0.0006	0.362	0.025	0.0593	0.0039	279	314	579
NAM10: Diorite															
1.1s	390	369	0.95	81	0.000198	0.35	0.1781	0.0050	1.870	0.088	0.0762	0.0026	1057	1071	1099
2.1c	377	82	0.22	62	0.000467	0.83	0.1694	0.0049	1.675	0.104	0.0717	0.0037	1009	999	978
2.2r	569	169	0.30	90	0.000216	0.39	0.1584	0.0048	1.607	0.063	0.0736	0.0016	948	973	1030
3.1s	301	65	0.22	52	0.000053	0.09	0.1742	0.0054	1.816	0.087	0.0756	0.0025	1035	1051	1084
4.1c	160	142	0.89	32	0.000085	0.15	0.1717	0.0068	1.778	0.076	0.0751	0.0009	1021	1037	1072
4.2r	410	102	0.25	65	0.000003	0.01	0.1616	0.0043	1.669	0.046	0.0749	0.0003	966	997	1066
5.1s	265	223	0.84	51	0.000047	0.08	0.1704	0.0058	1.784	0.065	0.0759	0.0006	1014	1040	1093
6.1c	330	249	0.75	64	0.000071	0.12	0.1729	0.0055	1.785	0.060	0.0749	0.0006	1028	1065	1065

Table 5: Cont.

NAM10: cont.	Grain.spot	U(ppm)	Th(ppm)	Th/U	Pb*(ppm)	204Pb/206Pb	% 206	206Pb/238U	±	207Pb/235U	±	207Pb/206Pb	±	AGES (in Ma)			
														206Pb/238U	207Pb/235U	207Pb/206Pb	±
6.2r	462	129	0.28	79	0.000038	0.06	0.1746	0.0050	1.798	0.057	0.0747	0.0007	1037	1045	1061	20	98
7.1c	168	94	0.56	32	0.000173	0.30	0.1774	0.0050	1.798	0.062	0.0735	0.0012	1053	1045	1028	35	102
7.2r	577	232	0.40	105	0.000038	0.07	0.1769	0.0060	1.821	0.064	0.0747	0.0003	1050	1053	1060	8	99
10.2s	269	239	0.89	56	0.000066	0.11	0.1823	0.0034	1.859	0.043	0.0740	0.0008	1080	1067	1040	22	104
12.1c	127	111	0.88	26	0.000010	0.02	0.1777	0.0036	1.801	0.044	0.0735	0.0009	1054	1046	1028	24	103
12.2r	331	85	0.26	57	0.000057	0.10	0.1746	0.0032	1.774	0.039	0.0737	0.0007	1038	1036	1033	19	100
13.1s	119	106	0.89	23	0.000010	0.02	0.1664	0.0039	1.670	0.047	0.0728	0.0010	992	997	1008	28	98
14.1s	171	151	0.89	35	0.000036	0.06	0.1779	0.0037	1.828	0.044	0.0745	0.0007	1055	1056	1056	19	100
15.1fr	339	82	0.24	59	0.000010	0.02	0.1779	0.0033	1.804	0.039	0.0736	0.0006	1055	1047	1029	17	103
15.2c	175	130	0.74	34	0.000066	0.11	0.1734	0.0038	1.782	0.046	0.0745	0.0008	1031	1039	1055	23	98
NAM11: Hypersphenite																	
1.1c	278	188	0.68	64	0.000248	0.44	0.2063	0.0059	2.365	0.095	0.0831	0.0020	1209	1232	1272	49	95
1.2r	1152	100	0.09	182	0.000216	0.39	0.1673	0.0046	1.700	0.055	0.0737	0.0010	997	1008	1033	28	97
2.1s	409	170	0.42	73	0.000470	0.84	0.1753	0.0055	1.713	0.084	0.0709	0.0024	1041	1014	955	71	109
3.1s	441	186	0.42	76	0.000542	0.97	0.1692	0.0049	1.745	0.107	0.0748	0.0038	1008	1026	1064	105	95
4.1c	449	310	0.69	79	0.001425	2.54	0.1512	0.0043	1.563	0.109	0.0750	0.0045	908	956	1068	125	85
4.2r	1390	116	0.08	223	0.000024	0.04	0.1696	0.0049	1.705	0.053	0.0729	0.0005	1010	1011	1012	15	100
5.1s	384	150	0.39	67	0.000583	1.04	0.1709	0.0058	1.729	0.093	0.0734	0.0028	1017	1019	1024	78	99
6.1c	229	147	0.64	60	0.000895	1.60	0.2367	0.0076	3.155	0.159	0.0967	0.0034	1370	1446	1561	67	88
6.2r	840	92	0.11	117	0.000374	0.67	0.1461	0.0051	1.430	0.065	0.0710	0.0018	879	902	958	53	92
7.1s	529	289	0.55	101	0.000089	0.15	0.1801	0.0048	1.853	0.053	0.0746	0.0006	1068	1065	1059	16	101
8.1c	620	84	0.13	114	0.000127	0.22	0.1910	0.0067	2.042	0.079	0.0775	0.0010	1127	1130	1135	24	99
8.2r	696	101	0.14	115	0.000024	0.04	0.1725	0.0041	1.767	0.045	0.0743	0.0005	1026	1034	1050	13	98
9.1s	468	212	0.45	88	0.000060	0.10	0.1805	0.0043	1.850	0.048	0.0744	0.0006	1070	1064	1051	17	102
10.2s	346	95	0.27	58	0.000022	0.04	0.1680	0.0033	1.732	0.047	0.0748	0.0012	1001	1020	1062	32	94
11.3r	606	80	0.13	101	0.000010	0.02	0.1750	0.0033	1.772	0.035	0.0734	0.0003	1039	1035	1026	9	101
12.2s	416	166	0.40	75	0.000001	-	0.1754	0.0033	1.793	0.037	0.0741	0.0005	1042	1043	1045	13	100
13.2c	212	140	0.66	47	0.000003	0.01	0.2040	0.0042	2.244	0.055	0.0798	0.0008	1197	1195	1191	21	101
13.3r	583	76	0.13	99	0.000036	0.06	0.1782	0.0033	1.800	0.036	0.0733	0.0004	1057	1045	1021	12	104
14.2s	380	189	0.50	69	0.000001	-	0.1724	0.0032	1.765	0.035	0.0743	0.0004	1025	1033	1049	11	98
17.1c	525	208	0.40	98	0.000087	0.15	0.1802	0.0034	1.932	0.041	0.0778	0.0006	1068	1092	1141	15	94

Notes:

(1) Uncertainties are at the one sigma level

(2) - signifies no 204Pb detected

(3) %206 = common 206Pb as a percentage of total 206Pb

(4) * = radiogenic Pb

(5) Zircon types: c = core; r = overgrowth; s = homogenous, structureless grain.

(6) %Conc = percentage concordancy

Zircons from the Koperberg Suite hypersthenite (NAM11), which intrudes both diorite and anorthosite, are identical in habit to those in the diorite although there are even fewer composite grains in the hypersthenite (Fig. 3). Three of the analysed zircon cores are clearly xenocrystic yielding $^{207}\text{Pb}/^{206}\text{Pb}$ ages of 1135 ± 24 , 1272 ± 49 and 1561 ± 67 Ma. The remaining analyses of structureless grains and overgrowths yield $^{207}\text{Pb}/^{206}\text{Pb}$ ages of **1028 ± 11 Ma** and **1049 ± 15 Ma**, but with the current data set it is impossible to distinguish between the two sub-populations on statistical grounds. A combined weighted mean $^{207}\text{Pb}/^{206}\text{Pb}$ age of **1037 ± 8 Ma** (Fig. 8c) is obtained, which is consistent with the fact that it intrudes the NAM10 diorite. The overgrowths, however, have the low Th/U signature recognised in other rock units of the OCD, interpreted as the distinctive signature of metamorphic growth of zircon. The age calculated for the hypersthenite zircon overgrowths is also recorded in a number of the other rock units analysed and signifies the peak granulite facies overprint of the region. Zircons typified as *structureless* in the hypersthenite sample have Th/U ratios normal for magmatic growth. This unit is, therefore, regarded as having been emplaced at **1037 ± 8 Ma**, at a time which is coeval with the mid-crustal thermal perturbation responsible for the peak of prograde granulite facies metamorphism in the region.

It is pertinent at this stage to compare the results obtained in the present study with the SHRIMP U -Pb zircon study by Clifford et al. (1995) on a Koperberg Suite anorthosite which intrudes the Nababeep gneiss. This study also recognised a well-defined xenocrystic core population at 1197 ± 15 Ma and a rim population at 1029 ± 10 Ma, both statistically indistinguishable from the cores and rims analysed in the present study. The rim population of Clifford et al. (1995) is, however, interpreted as magmatic, and thought to represent the age of emplacement of the anorthosite intrusion. As shown above, however, the anorthosite of the present study is intruded by both diorite and hypersthenite which yield ages of 1062 and 1040 Ma respectively. An alternative to Clifford's et al. interpretation, therefore, is that both anorthosite intrusions were emplaced at, or just before, 1062 Ma, but this event is not recorded in the dating because no magmatic zircon grew in the anorthositic parental magma. The anorthositic magma nevertheless picked up abundant xenocrystic zircon which acted as nuclei for zircon overgrowths during the regional metamorphic peak between 1060 and 1030 Ma. This interpretation will be correct if all anorthosites in the OCD are intruded by (and pre-date) diorite and hypersthenite whose ages are genuinely 1060-1040 Ma. If, however, Koperberg Suite emplacement was regionally episodic, and if there was more than just a single generation of anorthosite emplacement, then it is possible that anorthosites were also emplaced episodically between 1060 and 1030 Ma. It is also conceivable that some anorthosites in the region are unrelated to the Koperberg Suite, and may be around 1200 Ma in age. Such anorthosites contain the D₂ fabric and are invariably associated with orthogneisses of the Little Namaqualand Suite (A. Kisters, per. commun. 1995).

DISCUSSION and CONCLUSIONS

Events in the Okiep Copper District

A diagrammatic summary of the sequence of events in the OCD, as recorded in the SHRIMP U -Pb zircon ages from this study, is presented in Figure 9. The orthogneisses of the Gladkop Suite, in the northern portion of the OCD and dated at 1822 ± 36 Ma, record the only major remnant of Kheisian crust in the area. These rocks are at present mainly in amphibolite facies (Fig. 1) and petrographic evidence for their metamorphic pre-history is lacking. However,

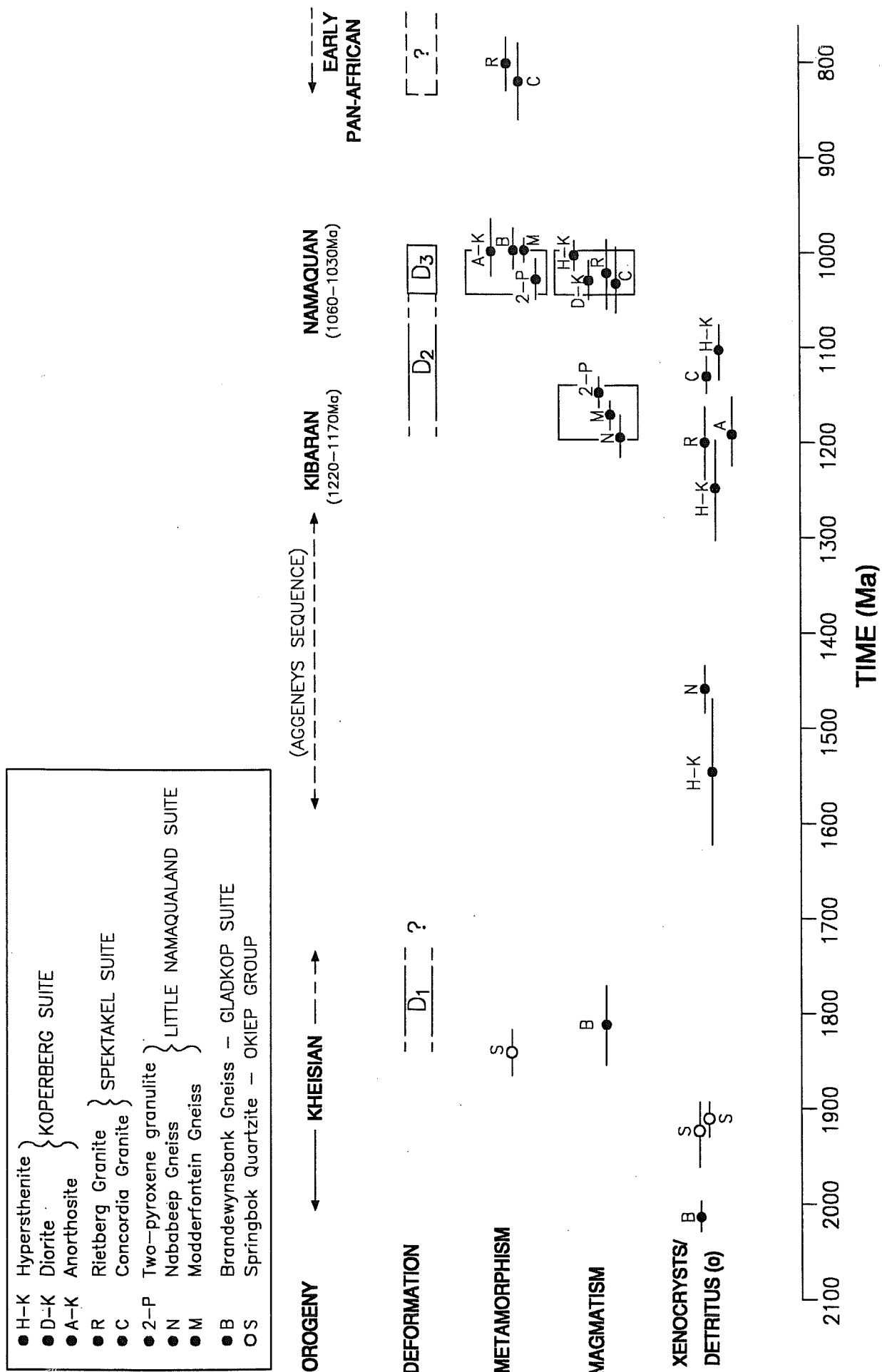


Fig. 9: A summary of the sequence of events in the Okiep Copper District as recorded in the SHRIMP U - Pb zircon dates of the present study.

evidence for even older Kheisian crust is present in the form of xenocrystic zircon cores from the Brandewynsbank orthogneiss, as well as from detrital grains in Khurisberg Group quartzites (also sampled in the OCD; Robb et al., in preparation). These provide ages of around 2020, 1940 and 1920 Ma (Fig. 9), which are similar to previously published whole rock isochron ages for the Orange River Sequence (Table 1). In addition, detrital grains in the Khurisberg quartzite sample are almost always characterised by overgrowths which collectively record a well-defined concordia intercept age of 1850 Ma. The age of these rims provides evidence of a metamorphic overprint (Fig. 9) in the Kheisian source rocks which supplied the detritus to the Khurisberg Group (Robb et al., in preparation).

Although two xenocrystic zircon cores record ages around 1500 Ma (Fig. 9), little else is preserved in the U -Pb zircon dating record in the OCD until a major pulse of magmatism associated with the Kibaran Orogeny. This magmatism is represented by intrusion of the voluminous Nababeep (at 1212 ± 11 Ma) and Modderfontein (at 1199 ± 12 Ma) orthogneisses, as well as a mafic sill (at 1168 ± 9 Ma). The regionally significant D₂ deformation either accompanied or immediately post-dated this event and possibly persisted until the Namaquan (Fig. 9). Alternatively, the D₂ deformation may comprise two discrete events, D_{2a} and D_{2b}, as suggested by Raith and Harley (1997), with the precise timing of the two events being still unclear. The abundance of xenocrystic zircon cores, which record ages of between 1140-1270 Ma (Fig. 9), within the younger Spektakel and Koperberg Suites also reflects the widespread development of Kibaran crust in the OCD.

A second major pulse of magmatism is associated with what is referred to here as the Namaqua Orogeny, between 1065-1030 Ma. This event was initiated by the intrusion of voluminous, sheet-like bodies of granite (the Spektakel Suite) at 1064-1058 Ma into open space created parallel to recumbent D₂ fabrics and lithologies. A compressional stress regime persisted with the onset of D₃, to form open folds and accompanying fabric rotation resulting in the development of the steep structures. It is these structures which were the preferred sites of emplacement of the Koperberg Suite intrusions at 1060-1040 Ma (Fig. 9).

Granulite facies metamorphism in the NMC is known from petrographic evidence to have post-dated or outlasted the D₂ deformation. The widespread development of zircon rims in rocks of the Gladkop and Little Namaqualand Suites dated at 1060-1030 Ma, and the fact that metamorphic and magmatic zircon domains in rocks of the 1060-1030 Ma Spektakel and Koperberg Suites are essentially indistinguishable, indicates that the metamorphic peak which accompanied zircon overgrowth occurred at the same time as the Namaquan magmatic event. There appears, therefore, to be a causative relationship between magmatism and metamorphism in OCD and this is discussed in more detail later on. It is also likely that the climax of granulite facies metamorphism in the region was at 1030 Ma since this is the age recorded in the majority of zircon rims.

Other metamorphic effects are also recorded in the zircon age data besides the widespread 1030 Ma granulite facies overprint. In the Nababeep gneiss several zircon overgrowths appear to define a Pb-loss discordia chord between ca. 1200 and 1000 Ma (Fig. 6A) suggesting that they actually formed as a result of contact metamorphism by the nearby intrusive Modderfontein orthogneiss, and then lost Pb during the regional granulite facies overprint. In the Spektakel Suite, zircon overgrowths are largely 860-840 Ma and these appear to define a metamorphic overprint of less severe magnitude or restricted extent. A possible

candidate for this might be related to the onset of an early Pan-African, amphibolite grade, overprint which becomes evident in the coastal belt to the west of the OCD.

The pattern of events recorded in the OCD is not entirely consistent with trends in other parts of the Mesoproterozoic orogenic belts of southern Africa. In southern Namaqualand, the Steenkampskaal monazite vein deposit, located in an apparent D₃ "steep structure", has been dated at about 1150±15 Ma (Andreoli et al., 1994). Thomas et al. (1995), however, also record the presence of a later magmatic event in southern Namaqualand in the form of the Bloukop granite, a Spektakel Suite correlative, and provisionally dated at 1060 Ma. Resolution of the sequence of events in the upper granulite facies terrane of southern Namaqualand awaits the successful dating of the migmatitic leucosomes which are unequivocally related to the metamorphic peak in this region (Waters, 1988; in preparation).

Recent dating in other portions of the Mesoproterozoic of Africa, such as Natal, also suggest that crustal growth might have occurred in two discrete episodes at 1220-1170 Ma and 1060-1030 Ma, and that this feature may, therefore, be characteristic of a much broader area than just the OCD. The voluminous rapakivi-textured granitoids (Oribi Gorge Suite) that underlie much of the Natal Metamorphic Complex have been dated at 1068-1029 Ma (Thomas et al., 1993), while other orogenic granitoids which pre-date these, but have not been accurately dated, appear to be around 1200 Ma. In the Kirwanveggen, Sverdrupfjella and Heimfrontfjella regions of Mesoproterozoic Antarctica, however, the situation is apparently more complex and a major event of zircon growth/overgrowth appears to have taken place rather at around 1150-1100 Ma (Arndt et al., 1991; Harris et al., 1995), with little or no record of the discrete Kibaran and Namaquan events described above.

Crustal growth

The review of Kibaran tectonic evolution in southern Africa by Thomas et al. (1994) is used as the basis for describing the pattern of crustal growth in the OCD as evident in the present study. Continental crust in pre-Kibaran times comprised the amalgamated Archaean Kaapvaal-Zimbabwe Craton which had accreted onto its western and south-western flanks a complex 2000-1800 Ma Kheisian terrane whose origin is still not fully understood (Hartnady et al., 1985; Thomas et al., 1994). In western Namaqualand, north of the OCD, a pristine, relatively unmetamorphosed, remnant of this crust (the Richtersveld terrane) is preserved as the Vioolsdrif Suite and Orange River Sequence, comprising a calc-alkaline composite batholith and associated extrusives perhaps akin to a magmatic arc adjacent to a convergent continental margin (Reid and Barton, 1983). The southern margin of the Richtersveld terrane is marked by the southward-verging Groothoek thrust, on the footwall side of which the largely amphibolite-grade Gladkop Suite orthogneisses are located. The region south of the Groothoek thrust is made up largely of potassic, high-SiO₂ orthogneisses of distinctly peraluminous character, some of which were emplaced at 1822±36 Ma (Fig. 5). Although the available initial ⁸⁷Sr/⁸⁶Sr ratio (R_0) is relatively low (i.e. 0.705±2; Barton, 1983) the suite is interpreted as having been an S-type granite which underwent gneissification very early on in its crustal history (Reid and Barton, 1983). Segments of the Kheisian crust were apparently metamorphosed at around 1850 Ma, as suggested by the age of zircon rims on detrital grains in Khurisberg Group quartzites (Fig. 9). The pre-Kibaran crust in the OCD, therefore, comprised segments of Richtersveld and Gladkop material, the only remnants of which are now preserved as tectonically interleaved slices, or digested components reflected in the xenocrystic zircon population. In addition, a

volcano-sedimentary supracrustal package, the Aggeneys Sequence, was also deposited sometime between 1600-1300 Ma (Table 1), possibly in response to rifting of the existing continent and deposition in extensional, intracratonic basins (Moore et al., 1990; Thomas et al., 1994).

Kibaran crustal formation in the OCD was initiated at about 1210 Ma by the intrusion of the Nababeep orthogneiss (and its correlatives) over a wide area, followed by intrusion of the Modderfontein orthogneiss over a more restricted area at 1200 Ma. The Little Namaqualand Suite is characterised by a high R_O of 0.725 ± 3 (Barton, 1983) and is generally believed to represent the partial melt products of older Proterozoic crust. The age and origin of this protolith is uncertain since the present study did not reveal the widespread presence of Kheisian-aged zircon xenocrysts in the samples analysed (Fig. 9). Geochemical modelling by McCarthy (1976) suggested that these orthogneisses were the residues left after various increments of melt had been extracted from them. Conversely, Reid and Barton (1983) viewed the rocks as an accumulated melt fraction derived during progressive partial fusion of a crustal source rock well below the present level of exposure of the OCD (since the NMC records limited evidence of *in situ* anatexis and migmatisation; Waters, 1988), with certain components also recording the effects of *in situ* crystal fractionation. It seems likely that Kibaran anatexis might have been associated with crustal thickening and the onset of convergence characterised by the D₂ deformation, reflecting the collision between Kheisian crust and the Kaapvaal-Zimbabwe Craton (Thomas et al., 1994).

Crustal formation during the Namaqua Orogeny was manifest in the emplacement of the extensive Spektakel Suite granites and the Koperberg Suite in the interval 1060-1030 Ma. The Concordia granite is a potassic, marginally peraluminous, high-SiO₂ intrusion with a markedly negative, crustal, ε_{Nd} signature (-7; Clifford et al., 1995), but relatively primitive R_O (0.709 ± 3). Raith (1995) regarded the suite as typically S-type in derivation, a feature consistent with its chemistry and association with tungsten mineralisation, but does not discount the possibility of contribution from A- or I-type magmatic precursors. McCarthy (1976) has pointed to the markedly differentiated trace element chemistry of the suite and suggested that *in situ* feldspar fractionation has taken place within the intrusions. The Concordia granite was emplaced in very late D₂ time, but prior to D₃, since many steep structures occur within it.

The Koperberg Suite is characterised by a variety of lithologies which include andesine anorthosite, biotite diorite, leuconorite, norite and hypersthene. The sequence of intrusion of the members of the suite exhibits a well-defined reversal of the normal differentiation trend suggesting either progressive partial melting or tapping of a differentiated magma chamber from the top downwards. As with most of the other rocks of the NMC the precursor to the Koperberg Suite has a distinctive crustal signature, with variable but high R_O (up to 0.727), high initial U/Pb ratio and a markedly negative ε_{Nd} signature (-9; Clifford et al., 1995). The latter workers have suggested that the Koperberg Suite was derived by partial melting of fertile (in terms of large-ion lithophile elements) lower crustal material of intermediate composition. Boer et al. (1994) and van Zweiten et al. (1996), on the other hand, favour a mantle origin for the mafic component of the suite and subsequent contamination by both wall rock and associated lower crustal melts. This model receives support from detailed Sr isotopic studies of the Koperberg Suite which points to a distinct bimodality in R_O (Brandriss, 1995). The presence of abundant xenocrystic zircon, particularly in the anorthosites (Clifford et al., 1995; Figs. 8 and 9)

which also have elevated R_O (0.725 as opposed to 0.710 for the more mafic units; Brandriss, 1996) certainly indicates that significant crustal contamination must have affected the more leucocratic components of the suite.

Gibson et al. (1996) recently proposed a model for the tectonic evolution of the OCD in which the Namaquan event is described as comprising a cycle of prograde metamorphism and compressive deformation (i.e. D₂ followed by D₃) culminating in the granulite facies climax. They recognise that it is improbable that a single deformation event could have persisted for more than 100 Ma and regard the deformation observed in the Concordia granite as late D₂. This view recognises no significant preservation of metamorphism or deformation related to the Kibaran Orogeny in the OCD. In reality, however, the geochemical character of the Little Namaqualand Suite is more compatible with a synorogenic setting than that of the Spektakel Suite. The microstructural evidence summarized by Waters (1989; 1990) indicates that D₂ deformation is intimately associated with the prograde metamorphism up to amphibolite grade, but that the granulite facies assemblages are essentially post-D₂. An alternative view is, therefore, proposed that the D₂ deformation and amphibolite facies prograde metamorphism is an integral part of the Kibaran orogenic cycle at around 1200 Ma. The discrete Namaquan event at 1060 - 1030 Ma comprises mainly a thermal pulse accompanied by the distinctive Spektakel and Koperberg magmatic suites, and by limited compressional deformation (D₃).

P -T -t path

The anticlockwise P -T -t path for the evolution of the granulite facies rocks of western Namaqualand (Waters, 1989) is well established, although the time constraints have depended on previously published whole rock Rb-Sr isotopic data whose relevance in terms of the metamorphic history of the region is now shown to be questionable. The onset of granulite facies metamorphism was previously assumed to coincide with the Rb-Sr errorchron age for the Little Namaqualand Suite (1187±22 Ma in Clifford et al., 1975 or 1223±48 Ma in Clifford et al., 1995) and to reflect the fact that these rocks were syn-orogenic, had been affected by the granulite facies overprint and, accordingly, had their Rb-Sr isotopic system re-set by the latter event. However, the Modderfontein orthogneiss, as well as other units in the region, clearly demonstrate zircon overgrowths at 1060-1030 Ma indicating that peak metamorphism was considerably later than ca. 1200 Ma. Rather than reflecting a metamorphic re-setting the Rb-Sr data for the Little Namaqualand Suite, and indeed other units in the region too, probably provide an imprecise indication of the true protolith age, a feature now known to be characteristic of many granulite facies terranes, where low aH_2O and restricted or closed system element mobility often result in preservation of original Rb-Sr isotopic systems. Comparison of previously published age data for the NMC (Table 1) with the age constraints provided in the present study illustrates a remarkable degree of first-order similarity.

The prograde P-T path for both lower and upper granulite facies rocks of the NMC (Fig. 1) is reconstructed in Figure 10 utilising the thermobarometric constraints summarized in Waters (1989) and the age data of the present study. The overall shape of the Namaquan P-T path is also likely to be anticlockwise since the emplacement of sheet-like granitoids of the Spektakel Suite, followed by D₃ deformation, would be expected to increase pressure at near-maximum temperature. The transition from amphibolite to lower granulite grades in the present model, as well as the transition from the D₂ to the D₃ stress regime, is considered to have

been accompanied by a major 100 million year hiatus between circa 1170 Ma and 1060 Ma (Fig. 10). The onset of the granulite facies prograde path was initiated, at around 1060 Ma, from the heat supplied by under- or intra-plating of mantle-derived basic magma, or by delamination of the lower lithosphere, or by both (Waters 1990; Gibson et al., 1996).

By contrast with the rapid onset of prograde metamorphism, the retrograde path appears to have been long-lived. Mineral reactions suggest isobaric cooling until around 600°C with subsequent decompression evident in the fact that kyanite is never observed as a retrograde mineral product. Whole rock ^{40}Ar - ^{39}Ar plateau ages of 790-845 Ma suggest that cooling and denudation of the Namaquan crust occurred as the result of some 4-8 km of uplift per 100 Ma (Clifford et al., 1995). This process may, however, have been interrupted or complicated by early Pan-African orogenic processes to the north-west of the OCD (i.e. the Gariep Belt; Fig. 1) which gave rise to zircon overgrowths at 850 Ma in certain rocks such as the H₂O-saturated Spektakel Suite (Raith, 1995). Subsequent uplift brought the present exposures of the OCD to the surface by about 600 Ma when the sediments of the Nama Group were unconformably deposited on the Kibaran/Namaquan crust.

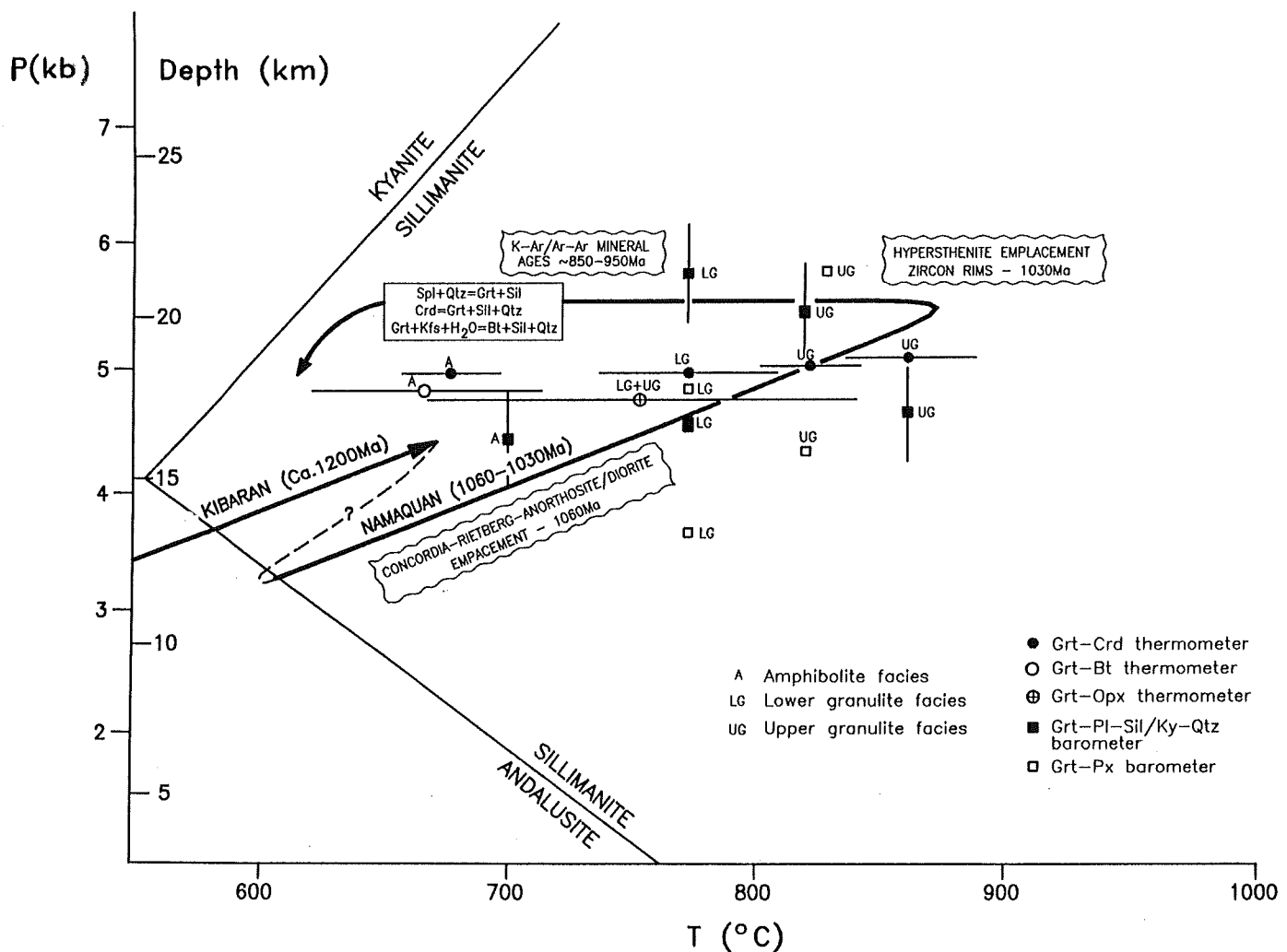


Fig. 10: Pressure-temperature-time path for the evolution of the Okiep Copper District during the Kibaran and Namaquan orogenies.

Causes of granulite facies metamorphism in the mid-crust

The evolution of granulite terranes along an anticlockwise, isobaric cooling path at relatively shallow levels in the crust (i.e. 5 kb or less) is a relatively uncommon feature (Harley, 1989) and requires a fairly specific explanation. Isobaric cooling from high temperatures in the mid-crust implies the existence of a significant thermal anomaly in continental material of normal, 25-40 km, thickness. Given the overall compressive stress regime of the OCD during the Kibaran and Namaquan orogenies, and the concurrence in ages between major magmatic pulses and metamorphic zircon growth in the area, it is likely that the origin of the granulite facies terrane in the western NMC is related to magmatic accretion into and under pre-existing continental crust accompanied by moderate crustal thickening (Waters, 1989; 1990). Other possible mechanisms such as extension of normal thickness crust with or without magmatic underplating, or extension of previously over-thickened crust (Harley, 1989), are inconsistent with the regional geological constraints.

Anticlockwise P-T-t paths in isobarically cooled granulites are recorded in rocks within or below the zone of magmatic accretion, but not above it. This is consistent with observations in the NMC where the prograde path is preserved in supracrustal assemblages of suitable compositions which occur at the same crustal level, or below, the zone occupied by the voluminous Spektakel Suite intrusions. However, the Spektakel and Koperberg suites are not sufficiently voluminous to account for the advected heat required, but are themselves symptomatic of a major increase in heat flux from depth. As suggested by Waters (1990) and Gibson et al. (1996) the heat is supplied either by under- or intra-plating of basic magma, or delamination of the lower lithosphere. Seismic refraction studies of the NMC have shown that the region is underlain, at depths greater than about 14 km, by a zone whose seismic velocities are consistent with a mafic (amphibolitic or dioritic) composition. The existence of a mafic underplate is also supported by the petrogenetic (AFC) characteristics of the Koperberg Suite and the development of the Spektakel Suite as a lower crustal anatect.

It remains to speculate on the cause of the thermal pulse 100-150 million years after the Kibaran convergence, magmatism and low-pressure amphibolite facies metamorphism. Although the fortuitous appearance of plume activity emerges as an initial solution, it does not account for the apparently widespread magmatic activity at the same time elsewhere in the extended Mesoproterozoic terranes of the region. Delamination at the base of a thickened lithosphere is another possible solution, but here too a problem arises in that the time gap is too great for the Namaquan event to be a direct consequence of Kibaran convergence. The plate tectonic setting of the region after the Kibaran collision is obscure although assemblies of the Rodinian supercontinent have been attempted (Hoffman, 1991; Dalziel, 1992). Two possible mechanisms for initiating a thermal event accompanied by moderate compression are:

- (1) renewal of subduction along the new outer edge of the continent, which lay presumably towards the south; and
- (2) stagnation following Kibaran collision and a change in the pattern of subduction leading to a build up of heat in the subcontinental mantle, and possibly also delamination of existing mantle lithosphere.

Whatever its cause, this thermal event was short-lived (ca. 30 million years) and was followed, after a further interval, by break up of the supercontinent along north-south trending

zones. A thermal pulse associated with ca. 850 Ma rifting may be recorded in the zircon overgrowths analysed from the Spektakel Suite. Alternatively, uplift and exhumation of crustal blocks occurring at this time may also be responsible for the ^{40}Ar - ^{39}Ar plateau ages of 790 - 845 Ma recorded in the western part of the OCD (Clifford et al., 1995).

The salient features associated with the development of mid-crustal granulite facies rocks in the OCD are summarized in Figure 11 which shows a schematic north-south section in Namaquan times. In this scheme, the metamorphic zonation of the region is related to the tectonic juxtaposition of the relatively unmetamorphosed Richtersveld terrane and the OCD along the south verging Groothoek shear, and the development of a subsequent granulite facies overprint in the thermally perturbed zone associated with the Namaquan magmatic accretion. The fact that there is no preserved record of granulite facies metamorphism recorded during the Kibaran (1212-1175 Ma) period of orogeny is perhaps related to the fact that there was no mafic underplate at this time and the thermal anomaly associated with granitoid magmatism of the Little Namaqualand Suite was insufficient for regional granulite grade metamorphism and zircon growth. Finally, it is unlikely that the 1060-1030 Ma Namaquan crust was substantially thickened by orogenic processes at this time because this would probably have resulted in noticeable decompression subsequent to the thermal climax as a result of isostatic readjustments. Instead, it is conceivable that the crust was thinned somewhat in the interval between Kibaran and Namaquan processes (i.e. between D₂ and D₃), perhaps in response to thermal relaxation after Little Namaqualand Suite emplacement, and that Namaquan accretion merely reinstated the crust to normal proportions.

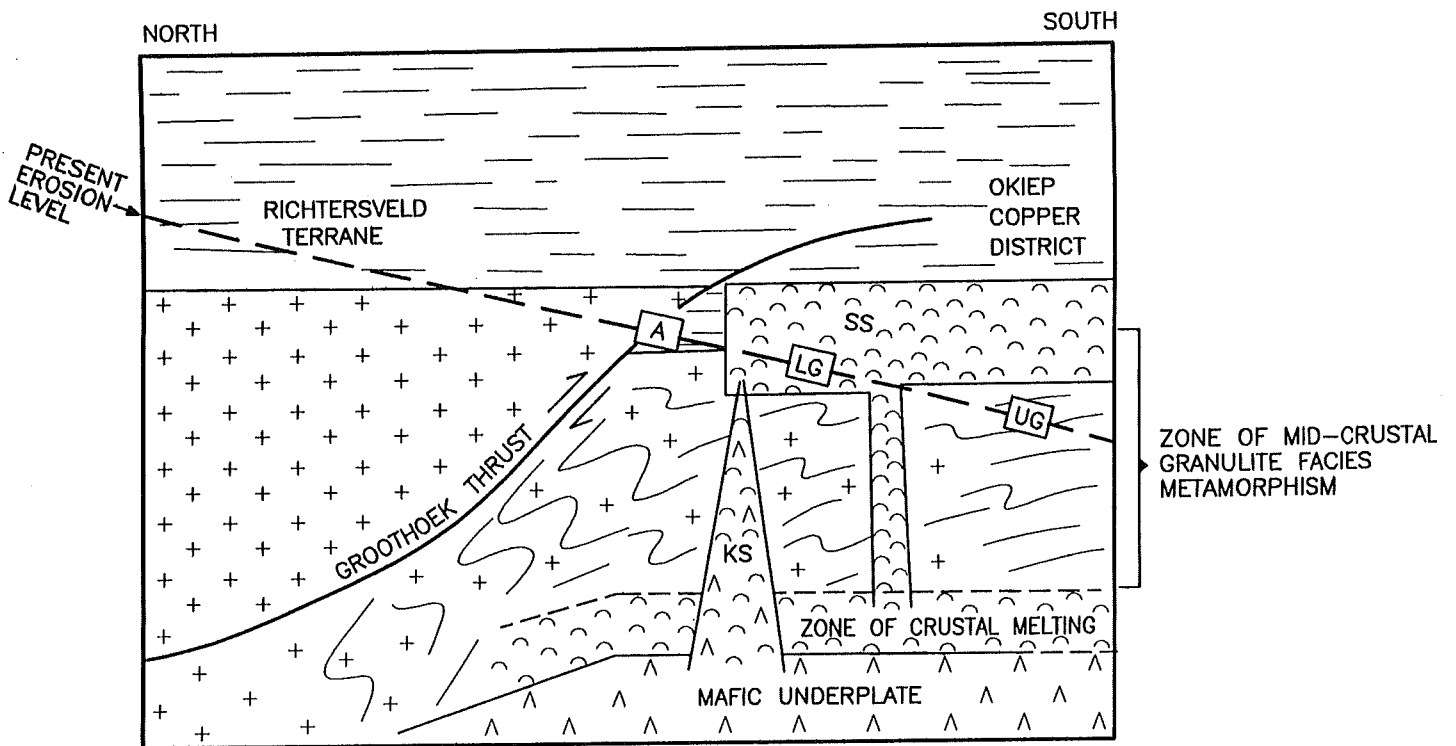


Fig. 11: Schematic model illustrating the mechanisms responsible for the development of mid-crustal granulite facies rocks in the Okiep Copper District.

ACKNOWLEDGEMENTS

Gold Fields of SA Ltd and the Foundation for Research Development (FRD) in South Africa are acknowledged for their logistic and financial support of this project. Sally Stowe and David Vowles of the ANU EM Unit are thanked for their assistance with the cathodoluminescence imagery.

REFERENCES

- Allsopp, H.L., Köstlin, E.O., Welke, H., Burger, A.J., Kröner, A. and Blignault, H.J. (1979). Rb-Sr and U-Pb geochronology of late-Precambrian early-Palaeozoic igneous activity in the Richtersveld (South Africa) and southern South West Africa. *Transactions of the Geological Society of South Africa* **82**, 185-204.
- Andreoli, M.A.G., Smith, C.B., Watkeys, M., Moore, J.M., Ashwal, L.D. and Hart, R.J. (1994). The geology of the Steenkampskaal Monazite Deposit, South Africa: implication for REE-Th-Cu mineralization in charnockite-granulite terranes. *Economic Geology* **89**, 994-1016.
- Arndt, N.T., Todt, W., Chauvel, M., Tapfer, M. and Weber, K. (1991). U-Pb zircon age and Nd isotopic composition of granitoids, charnockites and supracrustal rocks from Heimefrontfjella, Antarctica. *Geologische Rundschau* **80**, 759-777.
- Barton, E.S. (1983). Reconnaissance isotopic investigations in the Namaqua Mobile Belt and implications for Proterozoic crustal evolution - Namaqualand geotraverse. *Special Publication Geological Society of South Africa* **10**, 45-66.
- Blignault, H.J., Van Aswegen, G., Van Der Merwe, S.W. and Colliston, W.P. (1983). The Namaqualand geotraverse and environs: part of the Proterozoic Namaqua Mobile Belt. *Special Publication Geological Society of South Africa* **10**, 1-29.
- Boer, R.H., Meyer, F.M. and Cawthorn, R.G. (1994). Stable isotope evidence for crustal contamination and desulfidation of the cupriferous Koperberg Suite, Namaqualand, South Africa. *Geochemica et Cosmochimica Acta* **58**, 2677-2687.
- Brandriss, M.E. and Cawthorn, R.G. (1996). Formation of anorthosite and leucotonalite during magma hybridization in the Koperberg Suite of Namaqualand, South Africa. *South African Journal of Geology* **99**, 135-152.
- Clifford, T.N. (1970). The structural framework of Africa. In: Clifford, T.N. and Gass, I.G. (eds.) *African Magmatism and Tectonics*. Edinburgh, Oliver and Boyd, pp. 1-26.
- Clifford, T.N., Barton, E.S., Retief, E.A., Rex, D.C. and Fanning, C.M. (1994). A crustal progenitor for the intrusive anorthosite-charnockite kindred of the cupriferous Koperberg Suite, O'okiep District, Namaqualand, South Africa; new isotope data for the country rocks and the intrusives. *Journal of Petrology*, **36**, 231-258.

- Clifford, T.N., Gronow, J., Rex, D.C. and Burger, A.J. (1975). Geochronology and petrogenetic studies of high-grade metamorphic rocks and intrusives in Namaqualand, South Africa. *Journal of Petrology* **16**, 154-188.
- Clifford, T.N., Stumpf, E.F., Burger, A.J., McCarthy, T.S. and Rex, D.C. (1981). Mineral-chemical and isotopic studies of Namaqualand granulites, South Africa: a Grenville analogue. *Contributions to Mineralogy and Petrology* **77**, 225-250.
- Compston, W., Williams, I.S. and Meyer, C. (1984). U-Pb geochronology of zircons from Lunar Breccia 73217 using a sensitive high mass-resolution ion microprobe. *Journal of Geophysical Research* **89**, B525-B534.
- Cumming, G.L. and Richards, J.R. (1975). Ore lead isotope ratios in a continuously changing earth. *Earth and Planetary Science Letters* **28**, 1555-171.
- Dalziel I.W.D. (1991). Pacific margins of Laurentia and East Antarctica-Australia as a conjugate rift pair: evidence and implications for an Eocambrian supercontinent. *Geology* **19**, 598-601.
- De Villiers, J. and Sohnge, P.G. (1959). The geology of the Richtersveld. *Memoir of the Geological Society of South Africa* **48**, 266p.
- Dirks, P.H.G.M., Hand, M. and Powell, R. (1991). The P-T deformation path for a mid-Proterozoic, low-pressure terrane: the Reynolds Range, central Australia. *Journal of Metamorphic Geology* **9**, 641-661.
- Dirks, P.H.G.M. and Wilson, C.J.L. (1990). The geological evolution of the Reynolds Range, central Australia: evidence for three distinct structural-metamorphic cycles. *Journal of Structural Geology* **12**, 651-665.
- Gibson, R.L., Robb, L.J., Kisters, A.F.M. and Cawthorn, R.G. (1996). Regional setting and geological evolution of the Okiep Copper District, Namaqualand, South Africa. *South African Journal of Geology* **99**, 107-120.
- Green, R.W.E. and Durrheim, R.J. (1990). A seismic refraction investigation of the Namaqualand Metamorphic Complex, South Africa. *Journal of Geophysical Research* **95(B12)**, 19927-19932.
- Harley, S.L. (1989). The origins of granulites: a metamorphic perspective. *Geological Magazine* **126**, 215-247.
- Harris, P. D., Moyes, A.B., Fanning, C.M. and Armstrong, R.A. (1995). Zircon ion microprobe results from the Maudheim high-grade gneiss terrane, western Dronning Maud Land, Antarctica. *Extended Abstract Geocongress '95*, Geological Society of South Africa, 240-243.
- Hartnady, C., Joubert, P. and Stowe, C. (1995). Proterozoic crustal evolution in southwestern Africa. *Episodes* **8**, 236-244.

- Hoffman, P. F. (1991). Did the breakout of Laurentia turn Gondwanaland inside out? *Science* **252**, 1409-1412.
- Hoffman, P.F. (1992). Global Grenvillian kinematics and fusion of the Neoproterozoic supercontinent Rodinia. *Geological Association of Canada Program with Abstracts*, **17**, p.49.
- Jacobs, J., Thomas, R.J. and Weber, K. (1993). Accretion and indentation tectonics at the southern edge of the Kaapvaal Craton during the Kibaran (Grenville) orogeny. *Geology* **21**, 203-206.
- Joubert, P., (1971). The regional tectonism of the gneisses of part of the Namaqualand Metamorphic Complex. *Bulletin of the Precambrian Research Unit*, University of Cape Town **10**, 220p.
- Kisters, A.F.M., Potgieter, J.E., Charlesworth, E.G., Anhaeusser, C.R., Gibson, R.L. and Watkeys, M.K. (1994). Emplacement features of cupriferous noritoids in the Okiel Copper District, Namaqualand, South Africa. *Exploration and Mining Geology* **3**(3), 297-310.
- Köppel, V. (1978). Lead isotope studies of stratiform ore deposits of Namaqualand, NW Cape Province, South Africa, and their implications on the age of the Bushmanland Subgroup. *United States Geological Survey, Open File Report 78-701*, 223-226.
- Lombaard, A.F. (1986). The copper deposits of the Okiel District, Namaqualand. In: Anhaeusser, C.R. and Maske, S. (eds.) *Mineral Deposits of Southern Africa*. Geological Society of South Africa, Volume II, pp. 1421-1445.
- McCarthy, T.S. (1976). Chemical interrelationships in a low pressure granulite terrain in Namaqualand, South Africa, and their bearing on granite genesis and the composition of the lower crust. *Geochimica et Cosmochimica Acta* **40**, 1057-1068.
- Moore, J.M., Watkeys, M.K. and Reid, D.L. (1990). The regional setting of the Aggeneys/Gamsberg base metal deposits, Namaqualand, South Africa. In: Spry, P.G. and Bryndzia, T. (eds.) *Regional Metamorphism of Ore Deposits*. Utrecht VSP, 77-95.
- Raith, J.G. (1995). Petrogenesis of the Concordia Granite Gneiss and its relation to W -Mo mineralization in western Namaqualand, South Africa. *Precambrian Research* **70**, 303-335.
- Raith, J. G. and Harley, S. L. (1997). Low-P high-T metamorphism in the Okiel Copper District, western Namaqualand, South Africa. *Journal of Metamorphic Geology*, in press.
- Reid, D.L. (1979). Age relationships within the mid-Proterozoic Vioolsdrif batholith, lower Orange River region. *Transactions of the Geological Society of South Africa* **82**, 305-311.

- Reid, D.L. (1981). Sm-Nd ages from the Namaqua and Richtersveld provinces. *Extended Abstract, Geological Society of South Africa Geocongress '81*, Pretoria, 173-174.
- Reid, D.L., Welke, H.J., Erlank, A.J. and Betton, P.J. (1987). Composition, age and tectonic setting of amphibolites in the central Bushmanland Group, western Namaqualand Province, southern Africa. *Precambrian Research* **36**, 99-126.
- Reid, D.L. and Barton, E.S. (1983). Geochemical characterization of granitoids in the Namaqualand geotraverse. *Special Publication Geological Society of South Africa* **10**, 67-82.
- SACS (1980). Stratigraphy of South Africa. Part 1. L.E. Kent (Comp.). *Handbook Geological Survey of South Africa* **8**, 690p.
- Steiger, R.H. and Jager, E. (1977). Subcommission on geochronology: convention on the use of decay constants in geo- and cosmochronology. *Earth and Planetary Science Letters* **36**, 359-362.
- Tack, L., Duchesne, J-P., Liegeois, J-P. and Deblond, A. (1993). Two successive mantle-derived A-type granitoids in Burundi: Kibaran late-orogenic collapse and lateral shear along the edge of the Tanzanian craton. *Extended Abstract, 16th Colloquium of African Geology*, Swaziland, 353-355.
- Thomas, R.J., Agenbacht, A.L.D., Cornell, D.H. and Moore, J.M. (1994). The Kibaran of southern Africa: tectonic evolution and metallogeny. *Ore Geology Reviews* **9**, 131-160.
- Thomas, R.J., Eglington, B.M., Bowring, S.A., Retief, E.A. and Walraven, F. (1993). New isotope data from a Neoproterozoic porphyritic granitoid-charnockite suite from Natal, South Africa. *Precambrian Research* **62**, 83-101.
- Van Aswegen, G. (1983). The Gladkop Suite - the grey and pink gneisses of Steinkopf. *Special Publication Geological Society of South Africa* **10**, 31-44.
- Van Zweiten, A.J.M., McCarthy, T.S. and Cawthorn, R.G. (1996). A petrogenetic model for the Koperberg Suite: evidence from the Jubilee Mine, Namaqualand, South Africa. *South African Journal of Geology* **99**, 121-134.
- Waters D.J. (1986). Metamorphic zonation and thermal history of pelitic gneisses from western Namaqualand, S. Africa. *Transactions of the Geological Society of South Africa* **89**, 97-102.
- Waters, D.J. (1988). Partial melting and the formation of granulite facies assemblages in Namaqualand, South Africa. *Journal of Metamorphic Geology* **6**, 387-404.
- Waters, D.J. (1989). Metamorphic evidence for the heating and cooling path of Namaqualand granulites. In: Daly, J.S., Cliff, R.A. and Yardley, B.W.D. (eds.) *Evolution of Metamorphic Belts*. Special Publication Geological Society **43**, 357-363.

- Waters, D.J. (1990). Thermal history and tectonic setting of the Namaqualand granulites, southern Africa: clues to Proterozoic crustal development. In: Vielzeuf, D. and Vidal, Ph. (eds.). *Granulites and Crustal Evolution*. Kluwer Academic Publishers, The Netherlands, 243-256.
- Waters, D.J. (1991). Hercynite-quartz granulites: phase relations and implications for crustal processes. *European Journal of Mineralogy* **3**, 367-386.
- Waters, D.J., Joubert, P. and Moore, J.M. (1983). A suggested re-interpretation of Namaqua basement and cover rocks south and west of Bitterfontein. *Transactions of the Geological Society of South Africa* **86**, 86, 65-72.
- Welke, H.J., Burger, A.J., Corner, B., Kroner, A. and Blignault, H.J. (1979). U -Pb and Rb-Sr age determinations on middle Proterozoic rocks from the lower Orange River area, south-western Africa. *Transactions of the Geological Society of South Africa* **82**, 205-214.
- Williams, I.S. and Claesson, S. (1987). Isotopic evidence for the Precambrian provenance and Caledonian metamorphism of high grade gneisses from the Seve nappes, Scandinavian Caledonides. II Ion microprobe zircon U -Th -Pb. *Contributions to Mineralogy and Petrology* **97**, 205-217.

—oOo—

APPENDIX

SAMPLE DESCRIPTION AND LOCALITIES

(i) OKIEP GROUP

- NAM5 - Springbok Quartzite** (Khurisberg Subgroup)
 [Bulletrap Prospect road, north of Jan Coetzee Mine]
- NAM3 - 2-pyroxene granulite** (mafic sill intruding Nababeep gneiss)
 [Carolusberg West borehole CWS14, 384-388 metres]

(ii) GLADKOP SUITE

- NAM6 - Brandewynsbank orthogneiss**
 [type locality on the farm Brandewynsbank 17 km north of Okiel]
- NAM7 - Noenoemaasberg orthogneiss**
 [type locality on the farm Brandewynsbank 17 km north of Okiel]

(iii) LITTLE NAMAQUALAND SUITE

- NAM1 - Modderfontein orthogneiss** (intrudes Nababeep gneiss)
 [Narrap Mine borehole NR55, 235-270 metres]
- NAM2 - Nababeep orthogneiss**
 [Narrap Mine borehole NR55, 72-187 metres]

(iv) SPEKTAKEL SUITE

- NAM4 - Concordia granite**
 [Flat Mine North borehole FMN228, 36-120 metres]
- NAM8 - Rietberg granite**
 [Klein Nigramoep East borehole KNE6, 113-131 metres]

(v) KOPERBERG SUITE

- NAM9 - Anorthosite** (xenolith in diorite/hypersthenite)
 [Jubilee Pit]
- NAM10 - Biotite Diorite** (intruded by hypersthenite)
 [Jubilee Pit]
- NAM11 - Hypersthenite**
 [Jubilee Pit]

— oOo —